Earth's Future

RESEARCH ARTICLE
10.1029/2024EF005762

Special Collection:
Holocene climate changes: process, mechanism and impacts

Responses of the Natural Phytoplankton Assemblage to Patagonian Dust Input and Anthropogenic Changes in the Southern Ocean

Clément Demasy[1], Marie Boye[1], Ambroise Delisée[1], Jean-François Maguer[2], Melilotus Thyssen[3], and Léa Gest[4]

[1]Université Paris Cité, Institut de Physique du Globe de Paris, CNRS, Paris, France, [2]LEMAR, UMR 6539 UBO/CNRS/IRD, Institut Européen Universitaire de la Mer, Plouzané, France, [3]Aix Marseille University, Université de Toulon, CNRS, IRD, MIO, Marseille, France, [4]Université de la Réunion, Saint Denis, France

Abstract The cumulative effects of multi-faceted changes on the phytoplankton community of the Southern Ocean (SO) are not yet known, which is a major limitation to predicting the future direction of the biological carbon pump. Thus, our study aimed to estimate the effects of intensified Patagonian dust inputs, warming and acidification on the growth, composition and production of phytoplankton assemblages in the Polar Frontal Zone (PFZ) and the High-Nutrient Low-Chlorophyll (HNLC) region of the Indian sector of the SO during the austral summer 2022. Natural phytoplankton communities were incubated for 5-day under 4 scenarios (present and future conditions, and 2 intermediate scenarios). In the PFZ, +3°C and acidification stimulated the growth of phytoplankton, mainly cyanobacteria, while intensified dust inputs alone did not have notable impact. Conversely, in HNLC waters, the addition of Fe-dust alone increased the total chlorophyll *a* of diatoms (mainly *F. kerguelensis*), whereas the negative effect of acidification and +3°C counteracted the positive impact of dust input on the diatoms. In these waters, future conditions benefited smaller species (haptophytes and cyanobacteria). The net particulate organic carbon production (POC) was also unaltered by future conditions, suggesting that primary production may not change in the future SO. However the increase in the length and number of long-chain diatoms under future HNLC conditions may indicate that POC export could intensify in the future.

Plain Language Summary Phytoplankton in the Southern Ocean (SO) play a critical role in absorbing atmospheric carbon dioxide and supporting marine ecosystems, however their response to future environmental changes remains unclear. This study examined how increased dust inputs, warming, and acidification affect the phytoplankton community in two contrasted biogeochemical domains of the SO, the Polar Frontal Zone (PFZ) and the High-Nutrient Low-Chlorophyll (HNLC) region. In the PFZ, warming and acidification favored the smaller phytoplankton species, while in the HNLC region, iron-rich dust stimulated diatom species, though this effect was attenuated by warming and acidification. While overall the production of organic carbon by phytoplankton remained unchanged, diatoms may enhance carbon export to deeper waters under future conditions due to increased number and length of chain-forming species. These findings highlighted the complexity of phytoplankton responses, which vary across regions and are influenced by interactive environmental factors. Understanding the impact of these environmental factors on phytoplankton is critical to predicting how future changes will shape the role of the SO in the global carbon cycle.

Key Points:

- Warming and acidification stimulate cyanobacteria in the PFZ
- Fe-dust enhances diatom growth in HNLC waters
- Future conditions will not cause a change in carbon and nitrogen particulate production in PFZ and HNLC waters

Correspondence to:
C. Demasy,
demasy@sun.ac.za

Citation:
Demasy, C., Boye, M., Delisée, A., Maguer, J.-F., Thyssen, M., & Gest, L. (2025). Responses of the natural phytoplankton assemblage to Patagonian dust input and anthropogenic changes in the Southern Ocean. *Earth's Future*, *13*, e2024EF005762. https://doi.org/10.1029/2024EF005762

Received 8 JAN 2025
Accepted 7 MAY 2025

Author Contributions:
Conceptualization: Clément Demasy, Marie Boye
Data curation: Clément Demasy, Marie Boye, Ambroise Delisée, Léa Gest
Formal analysis: Clément Demasy, Marie Boye, Jean-François Maguer, Melilotus Thyssen
Funding acquisition: Marie Boye
Investigation: Clément Demasy, Marie Boye
Methodology: Clément Demasy, Marie Boye
Project administration: Marie Boye
Resources: Clément Demasy
Software: Clément Demasy
Supervision: Marie Boye
Validation: Clément Demasy, Marie Boye
Visualization: Clément Demasy
Writing – original draft: Clément Demasy

1. Introduction

The Southern Ocean (SO) is the largest High-Nutrient Low-Chlorophyll (HNLC) area in the world, where the biological production is low despite abundant macronutrients (Moore et al., 2001). This paradox has been explained by the "iron hypothesis", according to which the very low iron (Fe) inputs in the HNLC area limit the phytoplankton growth, given the essential role of Fe in the metabolic processes of primary producers (Martin, 1990). Iron and other trace metals, present at exceedingly low concentrations in the SO, can originate from several sources. South of 35°S, the dominant sources of Fe in deep waters are sediments and hydrothermalism, while atmospheric dust deposition and ice near Antarctica are the major sources of Fe in surface waters (Jickells et al., 2005; Tagliabue et al., 2010). A study showed that one-third of the productivity in the SO is supported by dust deposition (Weis et al., 2024). At these high latitudes, the main source of dust is the Patagonian Desert, often referred to as the "Patagonia dust machine" (Ackert Jr, 2009; Li et al., 2008). This desert dust, transported over

Writing – review & editing:
Clément Demasy, Marie Boye, Ambroise Delisée, Jean-François Maguer, Melilotus Thyssen, Léa Gest

vast distances in the Atlantic and Indian sectors of the SO, can fertilize the surface waters, spatially and temporally alleviating the limitation of micro-nutrients, such as Fe (Mahowald et al., 2010). While the role of trace metals in supporting phytoplankton productivity in the SO is well-established, the broader context of environmental shifts brings additional complexities to understanding these impacts.

The Anthropocene has come to a turning point in the 21st century, characterized by fast and profound shifts in environmental balances (Lewis & Maslin, 2015). In this context, the SO plays a crucial role in regulating the global climate (Hauck et al., 2015). It is recognized as the world's largest region for atmospheric carbon sequestration through both physical and biological pumps (Rodgers et al., 2014). At the base of the biological carbon pump are photosynthetic micro-organisms (Ducklow et al., 2001), notably key groups like diatoms. These siliceous microphytoplankton that have been present in the ocean at least since the Early Cretaceous (Bryłka et al., 2023; Medlin et al., 1997) play a pivotal role in enhancing the efficiency of the biological carbon pump due to their large size (Martin et al., 2011; Tréguer et al., 2018). The efficiency of the biological carbon pump depends on critical factors facilitating phytoplankton metabolic processes under optimal conditions such as temperature, light, pH and the availability of micro- and macro-nutrients (Perez-Garcia et al., 2011). These drivers are tracked in the SO, with various scenario projections from the Intergovernmental Panel on Climate Change (IPCC) helping to understand future global changes (Pörtner et al., 2022). The SO is unique by its mosaic of biogeochemical areas and is undergoing diverse environmental alterations, including a projected 3°C temperature rise by 2,100, a decrease of 0.3 pH units, and increased atmospheric Fe inputs (Constable et al., 2014; Deppeler & Davidson, 2017; Meredith et al., 2019). In addition, it is also possible that a decrease in wind strength could lead to a decrease in dust inputs. However, studies indicate an intensification of wind strength in the SO and therefore a potential increase in inputs of bioavailable Fe in the future (Bronselaer et al., 2020). These changes have potential effects on the composition and productivity of phytoplankton communities. To understand the biological impacts of these environmental changes and their subsequent effects on the biological carbon pump (Boyd et al., 2024) as well as the feedback mechanisms on climate, it is crucial to simulate these multi-faceted changes (Boyd et al., 2019; Browning & Moore, 2023). Previous studies have primarily focused on the individual impacts of environmental changes. For instance, increases in temperature or light, or nutrient availability, have been shown to stimulate the growth of phytoplankton (Arrigo et al., 2010; Browning et al., 2021; Raven & Geider, 1988). Conversely, decreasing pH may have either positive or negative effects, depending on the phytoplankton community (Duncan et al., 2022; Trimborn et al., 2013). However, studies exploring the cumulative effects of such environmental changes are limited (Boyd et al., 2016; Trimborn, Brenneis, et al., 2017; Trimborn, Thoms, et al., 2017). These parameters can exhibit synergistic or antagonistic interactions, highlighting the need to investigate their multi-faceted effects in order to better understand the impact of future changes on phytoplankton in the SO (Glibert et al., 2020).

A realistic simulation of a biome and its ecosystem under environmental changes poses significant technical challenges. However, some studies have successfully replicated the biological responses of polar ecosystems under controlled and varying environmental conditions. For instance, a study examined the effects of acidification and Fe inputs, either in the form of inorganic Fe or Australian dust inputs, on the natural phytoplankton assemblage in the SO (Trimborn, Brenneis, et al., 2017). This study showed that the CO_2-dependent phytoplankton species shift was controlled by Fe sources. In both the control and dust treatments, the resulting phytoplankton communities were dominated by the same species, and ocean acidification led to a shift from diatoms to Prymnesiophyceae. Another study explored the combined effects of acidification, warming, increase of Fe concentration and photosynthetic active radiation (PAR), and decrease of macronutrients on a subantarctic diatom (Boyd et al., 2016). The findings indicated that the net effect of warming on increased growth of a subantarctic diatom would have been underestimated by about 15% if the interactive effects of other stressors were not considered (Boyd et al., 2016). This highlights that future projections can be biased when only a subset of multi-stressors is considered, emphasizing the need to conduct multi-factor experimental studies with the whole phytoplankton assemblage of the SO. A recent study compared the impact of two atmospheric sources (desertic and volcanic) on the phytoplankton community in the Indian sector of the SO (Geisen et al., 2022). Both atmospheric inputs were found sufficient to stimulate phytoplankton growth, particularly diatoms. Although volcanic dust induced a greater increase in phytoplankton growth compared to desert dust, the extent of this stimulation was more dependent on whether the deposition area was Fe-limited than on the composition of the dust itself. These previous studies examining the impacts of different environmental changes on the natural phytoplankton community in the SO have not considered all drivers of phytoplankton growth and have not

comprehensively simulated future conditions. Therefore, it is crucial to conduct additional experiments to forecast the future trajectory of growth, composition and production of the phytoplankton assemblage in the SO.

This study aimed to assess the individual and cumulative impacts of projected intensification of Patagonian dust input by 2,100 in conjunction with other environmental changes such as warming and acidification, on the natural phytoplankton assemblage of the SO. For this, onboard incubation experiments were conducted in the Indian sector of the SO, an area known for significant deposition of Patagonian dust (Demasy et al., 2024; Heimburger et al., 2013; Li et al., 2008), which have ratio close to those found in Patagonian dust (Demasy, 2023), compared to dust from Southern Africa (Gili et al., 2022), which settles at lower latitudes, and dust from Australia (Attiya & Jones, 2022), which is primarily deposited in the Pacific sector of the SO (Li et al., 2008). These incubations were conducted in the Polar Frontal Zone (PFZ) and the HNLC area, two distinct biogeochemical regions. The PFZ is characterized by significant seasonal variations, with a predominance of smaller species such as cyanobacteria and coccolithophorids (Franck et al., 2000; Le Moigne et al., 2013; Shramik et al., 2013). In contrast, the HNLC area is characterized by Fe limitation and high macronutrient concentrations, supporting the presence of larger species such as diatoms year-round (Armand et al., 2008; Le Moigne et al., 2013; Leblanc et al., 2005). Our study used a reduced factorial design to assess the impact of environmental changes in these two regions of the SO. The experimental setup encompassed both current and future conditions, mirroring changes projected by the IPCC (Boyd et al., 2016; Pörtner et al., 2022). This focus centered on three main drivers (dust input as the main factor, and temperature and pH as a combined stressors), along with two intermediate scenarios, to evaluate the interactions between these factors.

2. Material and Methods

2.1. Sampling of Surface Seawater

The natural phytoplankton assemblages were collected onboard the French *R.V. Marion Dufresne II* in the Indian sector of the SO during the summer 2022 (February). Samples were taken from two stations, one located in the PFZ (at 47°40S, 58°00'E; sampled on 02/16/2022), and the other in the HNLC area (at 56°30S, 63°00'E; sampled on 02/19/2022).

Seawater was collected at a depth of approximately 15 m using an ultra-cleaned PTFE diaphragm VA-P08 pump (VERDERAIR® PURE) operating at a flow rate of 15 L min^{-1}. To remove larger zooplankton grazers, the seawater was initially filtered through a 200 µm mesh (nylon). Filtration took place under a laminar flow hood within a clean space set up on the ship. Subsequently, 100 L of seawater was sampled at each station and distributed into cleaned 10 L polycarbonate (PC) bottles (Nalgene®) assigned to the various tested scenarios.

2.2. Protocols of Microalgae Incubations Under Different Scenarios

The selected stressors included the input of Patagonian dust as the target main driver, with temperature (T) and pH as combined drivers. Patagonian dust was selected as the main parameter in the factorial design, due to its significant contribution to phytoplankton production in the SO (Li et al., 2008; Shoenfelt et al., 2018; Weis et al., 2024; Wyatt et al., 2023). To streamline the experimental process, T and pH were combined, thereby reducing the overall number of experiments needed. Four distinct scenarios (Figure 1; Table 1) were simulated to reflect environmental conditions: (A) the current conditions for dust input, T and pH, (D) the projected future conditions for 2,100, and two intermediate scenarios (B and C). Scenario B represented future dust input conditions and current T and pH conditions, and scenario C represented the current dust inputs and future T and pH conditions. Each scenario was performed in duplicate experiments. Additionally, control experiments without dust addition were conducted at each station under present (TA) and future (TF) conditions of T and pH. This experimental design allowed us to assess both the individual impact of dust input and the combined effects of T and pH, as well as the interactions between these drivers.

The scenario parameters (Table 1) were selected based on IPCC projections for the SO (Boyd et al., 2016; Pörtner et al., 2022) and adapted to in situ conditions. For instance, the +3°C warming scenario is based on the in situ condition. Regarding pH, although there is difference between the two zones (Table 2), equilibration through gas exchange with a simulated future atmosphere (800 ppm CO_2) has resulted in a pH decrease and mimicked natural acidification.

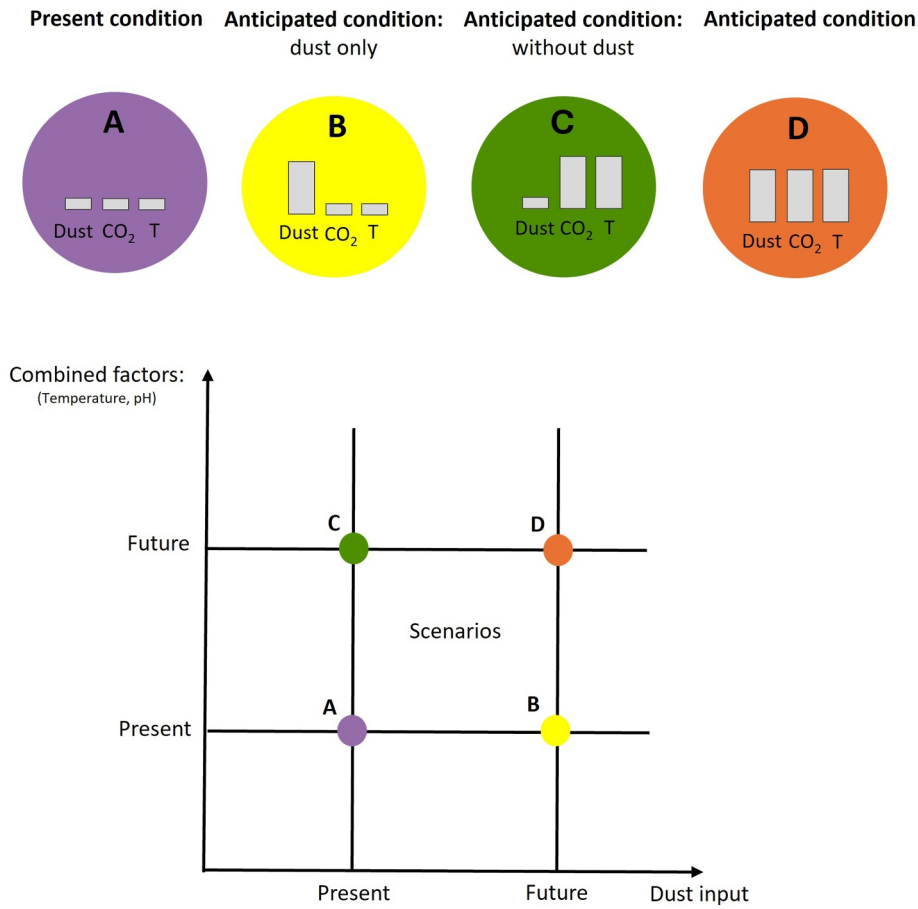

Figure 1. Diagram of scenario A (present condition), scenario B (future projection of dust and present condition of temperature and pH), scenario C (present input of dust and projection of warming and acidification), scenario D (projected condition).

To simulate seawater acidification (scenarios C and D, and TF), 500 mL seawater from a 10 L bottle was bubbled with a pure carbon dioxide (CO_2) gas (ALPHAGAZ® 1 purity) for 2 min. This seawater was then returned to the 10 L bottle (Riebesell et al., 2011). Subsequently, the 10 L bottle was then bubbled with a mixture of 800 ppm CO_2 gas (ALPHAGAZ® SAPHIR) until pH equilibration around 7.80. To ensure particle-free injection into the seawater, gases were injected through ultra-clean pipes and passed through 0.2 µm PTFE filters (Pall Acro-Vent™). The pH was measured using a pH probe (pHC281 HACH®) that has been calibrated with three reference buffer solutions at pH 4, 7 and 10 respectively, prior to use.

The dust was prepared in the land-laboratory by grinding Patagonian soil collected at 50.30°S–71.81°W. Pre-weighed amounts of 10 and 20 mg using a micro-balance (Mettler Toledo MX5®) were used to mimic the present (1 mg L^{-1}) and future (2 mg L^{-1}) dust input. The concentration for the present scenario was estimated based on regional conditions (Heimburger et al., 2013; Li et al., 2008), while the doubling in the future scenario was determined using atmospheric deposition projections (Gassó & Stein, 2007; Mahowald et al., 2010; Shi et al., 2023). Additionally, dust models and measurements lack the resolution to apply distinct dust fluxes to each zone. Prior to addition to the 10 L seawater bottle, the dust was mixed with a small volume of equilibrated seawater in a cleaned Eppendorf coning tube and then centrifuged using a portable centrifugation device (vortex genie 2 Scientific Industries®). Then, the dust was introduced into the 10 L bottle previously equilibrated at the target pH, vigorously shaken and then subdivided in 2 L polycarbonate bottles

Table 1
Incubation Experiments Were Conducted in Four Scenarios, Each Reflecting Distinct Experimental Conditions Performed in Duplicates

Scenario	Temperature (°C)	pH	Dust input (mg L^{-1})	PAR
A	in situ	in situ	1	in situ
B	in situ	in situ	2	in situ
C	+3	−0.3	1	in situ
D	+3	−0.3	2	in situ

Table 2
Physico-Chemical and Biological Parameters in the Ambient Seawater of the PFZ and HNLC Area Used for the Incubation Experiments (n = 2)

	PFZ	HNLC
Temperature (°C)	7.88	2.45
pH	8.13	7.96
Alkalinity (µmol L^{-1})	2,088 ± 47	2,122 ± 19
Nitrate (µmol L^{-1})	19.4 ± 0.69	27.5 ± 0.89
Silicate (µmol L^{-1})	7.78 ± 0.46	28.8 ± 0.58
POC (µmol L^{-1})	5.90 ± 1.15	4.99 ± 0.63
PON (µmol L^{-1})	0.75 ± 0.08	0.74 ± 0.09
PFe (µmol L^{-1})	6.96 ± 1.52	2.93 ± 1.55
Biogenic Si (µmol L^{-1})	0.012 ± 0.004	0.011 ± 0.006
Lithogenic Si (µmol L^{-1})	0.011 ± 0.006	0.006 ± 0.001
Chlorophyll *a* (µg L^{-1})	0.18 ± 0.01	0.26 ± 0.02
Total cell abundances (cells μL^{-1})	13.39 ± 1.05	5.08 ± 0.61
Nanophytoplankton (cells μL^{-1})	0.31 ± 0.10	0.20 ± 0.04
Picophytoplankton (cells μL^{-1})	13.08 ± 0.96	4.88 ± 0.60

(Nalgene®) for daily sampling. The PC bottles were cleaned 48 hr with 2% decon, 1 week in 10% HCl and stored until use in 2% distilled HCl.

The 2 L bottles were placed in two incubators covered by a 201 full CTB filter from Lee filter® on the ship's back deck exposed to natural light. One incubator simulated the current *T* conditions (scenarios A and B, and control TA) by maintaining an open circuit of surface seawater that was pumped continuously from the ship, reflecting the ambient surface temperature. The other incubator mimicked future *T* conditions, with the water flow regulated intermittently to adjust temperature. This was achieved using a thermostat connected to a temperature controller, which maintained the temperature at +3°C above the ambient conditions recorded in the first incubator. Temperature adjustments occurred at least twice a day, including once during the night. Since the ship was underway southwards from the PFZ station to the HNLC station and then ship back deck northwards, the ambient *T* decreased from 11.4°C to 3.9°C in the incubation with PFZ waters, and increased from 4.8°C to 15.5°C in the incubations with HNLC waters over the 5-day after seeding. Although this difference could introduce some bias to the study, polar phytoplankton groups have an optimal growth temperature range of 0–14°C, which practically covers the temperature variation being considered (Coello-Camba & Agustí, 2017). Moreover, the surface waters of the SO can fluctuate by up to 5°C throughout the year (Barnes et al., 2006; Chapman & Walsh, 2007; Morley et al., 2010) and a combination of wind and current forcing can lead to a cooling of up to 9°C (Leber et al., 2017). During the 5-day of incubation under TA conditions, in which no dust was added and the temperature varied according to the ambient conditions, the cell abundance and pigment concentration did not varied significantly in the PFZ waters (TChl *a* average = 0.18 ± 0.02 µg L^{-1}; cell abundance average = 13.22 ± 0.87 cells μL^{-1}). In contrast, variations were observed in the HNLC waters (TChl *a* average = 0.34 ± 0.18 µg L^{-1}; cell abundance average = 5.84 ± 2.84 cells μL^{-1}), where the end of the incubation was outside of the variance (TChl *a* = 0.64 µg L^{-1}; cell abundance = 16.36 cells μL^{-1}). However, these variations were additional to all scenarios and may not directly influence the scenario-specific effects. Since temperature fluctuations were recorded in the controls and were uniform across scenarios, the effects of dust input, acidification, and +3°C warming were assessed through direct comparisons. This study accounted for natural environmental variability, which could have partially masked treatment responses if it exceeded experimental effects. However, significant differences in cell abundance and photosynthetic biomass among scenarios (ANOVA: $p = 0.02$ in PFZ, $p = 0.01$ in HNLC) confirmed the robustness of our results. The TA control treatment, where temperature naturally varied, showed minor phytoplankton shifts, suggesting that cooling had little effect with the PFZ waters, while warming of the HNLC waters likely stimulated growth. Despite these background variations, phytoplankton responses to experimental treatments remained distinct, confirming that experimental treatments significantly impact phytoplankton communities. Given that natural variability influenced all treatments yet responses still differed, the observed effects may have been either underestimated (e.g., for PFZ cyanobacteria) or overestimated (e.g., for HNLC picoplankton). Every day, the 2 L bottles were sampled at maximum light (around noon) for each scenario and the controls. If pH changed over the course of the experiments in the acidification-mimicking scenarios, the 2 L bottles were further bubbled with 800 ppm CO_2 gas mixture. Sampling times during the incubation were designated as following: t-1 (before dust addition), t0 (at the time of dust addition), t1 (day 1), t2 (day 2), t3 (day 3), t5 (day 5).

2.3. Scanning Electron Microscope Analyses

A 50 mL volume was filtered through a PC filter holder (Nalgene®) with a PC filter (porosity of 0.2 µm, 47 mm Ø, Nuclepore™). The filter was then dried and stored at room temperature. To prepare the sample for microscopic examination, the filters were gold coated. Large phytoplankton species were observed during the experiments using a focused ion beam-scanning electron microscope (FEG-FIB-SEM) Auriga 40 from Zeiss®, fitted with a Zeiss Gemini column (Liu et al., 2016).

2.4. Taxonomic Identification

Taxonomic identification and enumeration of microphytoplankton (20–200 μm) and nanophytoplankton (3–20 μm) were carried out using an inverted microscope (WildM40) in samples preserved with neutral lugol solution (Dussart, 1992). Utermöhl settling chambers were used for microphytoplankton analyses (Hasle, 1988), and a smaller sedimentation chamber (2.97 mL) for the analyses of nanophytoplankton. Phytoplankton were identified to the lowest taxonomic level achievable (species, genus or group) using classical manuals for marine phytoplankton identification (In Scott & Marchant, 2005; Tomas, 1997) and the World Register of Marine Species database (WoRMS Editorial Board, 2023), while recognizing that certain taxa may require other higher-resolution techniques for definitive species-level identification. Biovolume of each species was also estimated from these microscope analyses (Hillebrand et al., 1999).

2.5. Flow Cytometry Analyses

A 2 mL sample was collected daily from each duplicated scenario and directly analyzed from a cryotube and stored in the dark. Analysis of cell density and estimated size were performed onboard using a CytoSense flow cytometer (CytoBuoy®) within a maximum of 2 hr after the sampling. A description of the instrument and the size conversion protocol can be found in Tulet et al., 2024. The instrument was calibrated with silicate beads of different sizes (1.0, 2.01, 3.13, 5.02, and 7.27 μm non-functionalized silica microspheres, Bangs Laboratories, Inc) to estimate particle size from the average pulse shapes of forward scatter per group, and to control measurement stability. Two distinct analysis protocols were implemented for each sample, one with a lower detection threshold (in ∼190 μL sample volume) to finely examine OraPicoProk (*Synechococcus*-like cells), and another one enabling higher detection threshold (in ∼1,800 μL sample volume) to analyze picoeukaryotes to nanophytoplankton cells. Additionally, the instrument was coupled with a camera specifically targeting large cells (>10 μm), improving the identification and differentiation of various phytoplankton groups. The raw data generated by the CytoUSB control software underwent processing using CytoClus 4 software. Cytograms which graphically display all cells counted in the sample according to the particle optical characteristics (scatters and emitted fluorescence), were employed for identifying phytoplankton groups. The total area under the curve of the sample was used for optimal cell signal representation. Group characterization was achieved by excluding background and comparative analysis. Post-processing of the cytograms yielded results that quantified the abundance (cells μL^{-1}) of distinct phytoplankton groups (Malkassian et al., 2011; Thyssen et al., 2022). The phytoplankton groups were classified and standardized according to the reference database F02 of Marine Microbial Flow Cytometry Standardised Group Names. The net growth rates (μ) were calculated according to Equation 1, with the slope of the cell density (N) as a function of incubation time (t).

$$\mu\left(d^{-1}\right) = \frac{\Delta Ln(N)}{\Delta t} \quad (1)$$

Abundance of microphytoplankton was not significant in the small volume analyzed, consequently, they were not presented.

2.6. Pigments Analyses

A 500 mL seawater sample was filtered from each duplicated scenario through a polysulfone filter (porosity of 0.7 μm, 25 mm Ø) using a filtration ramp with glass pump heads (25 mm Ø) connected to a vacuum pump. The filter was carefully folded into quarters with metal tweezers and stored in hemolysis tubes at −80°C until laboratory analysis. The filters were extracted in 100% methanol, ground and clarified by filtration (GF/F Whatman) over a period of 2 hr (Ras et al., 2008). The extract was analyzed by High-performance liquid chromatography (HPLC) Agilent Technologies 1,200. Carotenoids and chlorophyll *c* and *b* were detected at 450 nm, while chlorophyll *a* (Chl *a*) and its derivatives were identified at 676 nm and bacteriochlorophyll *a* at 770 nm. Quantitative computations to determine total Chl *a* (TChl *a*) for each phytoplankton group used the diagnostic pigments (DP) (Gieskes et al., 1988; Uitz et al., 2010). One limitation of using diagnostic pigments is their broad generalization; for example, Antajan et al. (2004) suggested that haptophyte contributions may be underestimated.

2.7. Particulate Carbon and Nitrogen Analyses

Two separate 350 mL samples of seawater were filtered using a filtration ramp with glass pump heads (25 mm Ø) connected to a vacuum pump. This filtration used GF/F filters (porosity of 0.7 µm, 25 mm Ø) previously calcined during 4 hr at 450°C and stored in calcined glass tubes. Filters were then frozen at −20°C until laboratory analysis. Upon returning to the laboratory, one of the two filters from each sample was decarbonated in glass vials and under concentrated HCl vapors within a glass desiccator for 4 hr at room temperature to analyze particulate organic carbon (POC) and nitrogen (PON). These filters were placed in a fume hood for 3 hr and then transferred to an oven at 60°C to remove residual HCl. For the analyses, the filters were placed in a tin capsule where they underwent combustion and reduction in a mass spectrometer (delta plus, Thermofisher, Bremen, Germany) which is coupled with a C and N analyzer (Flash EA, Thermofisher Scientific) via a type III interface. The analyses were calibrated using atropine OAS (SYLAB SARL®) standards. Accuracy of the analyses was 0.04% and 0.5% for N and C, respectively. Total particulate carbon (TPC) and total particulate nitrogen (TPN) were directly analyzed from the filters. By subtracting POC from TPC and PON from TPN, we determined particulate inorganic carbon (PIC) and particulate inorganic nitrogen (PIN). The net production rates of POC and PON were calculated (Equation 2) as the difference in concentrations between day 5 (C_{t5}) and the initial time (C_{t0}), divided by the incubation period ($\mathbf{\Delta}t$).

$$\text{Net production rate } \left(\mu\text{mol } L^{-1}\ d^{-1}\right) = \frac{C_{t5} - C_{t0}}{\Delta t} \quad (2)$$

2.8. Statistical Analyses

Significant differences between scenarios were assessed on the flow cytometry (FCM) and the HPLC data. An ANOVA test (Fisher, 1992) complemented by a Tukey test (Tukey, 1949) were performed using *R* software to analyze variations among scenarios.

A reduced experimental design was used, focusing on Patagonian dust as the primary parameter, while consolidating other environmental factors (pH, T) into a single parameter. These two factors were configured under present and future conditions, resulting in four distinct scenarios representing various combinations of the two parameters under different conditions. A statistical model employing a 2^2 factorial design (Goupy, 1993) was used to estimate the relative weight of each parameter (dust addition, and the combination of pH and temperature) and their interactions on changes in phytoplankton flow cytometry groups abundances and pigment concentrations.

3. Results

3.1. Biogeochemical Conditions in the Ambient Seawaters

The experiments were conducted during the late austral summer, following the seasonal phytoplankton bloom in the PFZ (Fiala et al., 2004). TChl *a* concentration was low in the surface waters of the PFZ (0.18 ± 0.01 µg L^{-1}, $n = 2$; Table 2) and phytoplankton size classes, assessed using the DP were primarily composed by 46% of nanophytoplankton (19'HF, 19'BF, Allo) and by 39% of picophytoplankton (Zea, TChl *b*). Pigments belonging mostly to microphytoplankton (Fuco, Perid) contributed a fraction of 15%. Among the pigments based on microphytoplankton class, a significant proportion of dinoflagellates was found, mainly represented by *Gymnodinium* sp. (93%) compared to diatoms, which were predominantly central diatoms (Figure 2c). The nanophytoplankton, identified as haptophytes (19'BF; Figure 3), was mainly constituted by coccolithophorids (Figures 2g and 2h), while the picophytoplankton encompassed prochlorophytes (Zeaxanthin and TChl *b*). The abundance counted by FCM of pico- and nano-phytoplankton was ∼13.2 cells µL^{-1}, with picophytoplankton being the predominant size-fraction accounting for up to 98% and nanophytoplankton 2%.

The concentrations of PIC and PIN in these waters were below detectable levels, preventing precise determination through the subtraction of the organic fraction from the total fraction. The concentrations of POC and PON were estimated at approximately ∼5.90 and ∼0.75 µmol L^{-1}, respectively (Table 2).

In the HNLC area, the TChl *a* concentration was also low (0.26 ± 0.02 µg L^{-1}) (Table 2). In contrast to the PFZ, microphytoplankton based on the DP, dominated the natural phytoplankton community, accounting for about 56% of the TChl *a* concentration, with *Fragilaropsis kerguelensis* (Figures 2a and 2b) being the predominant

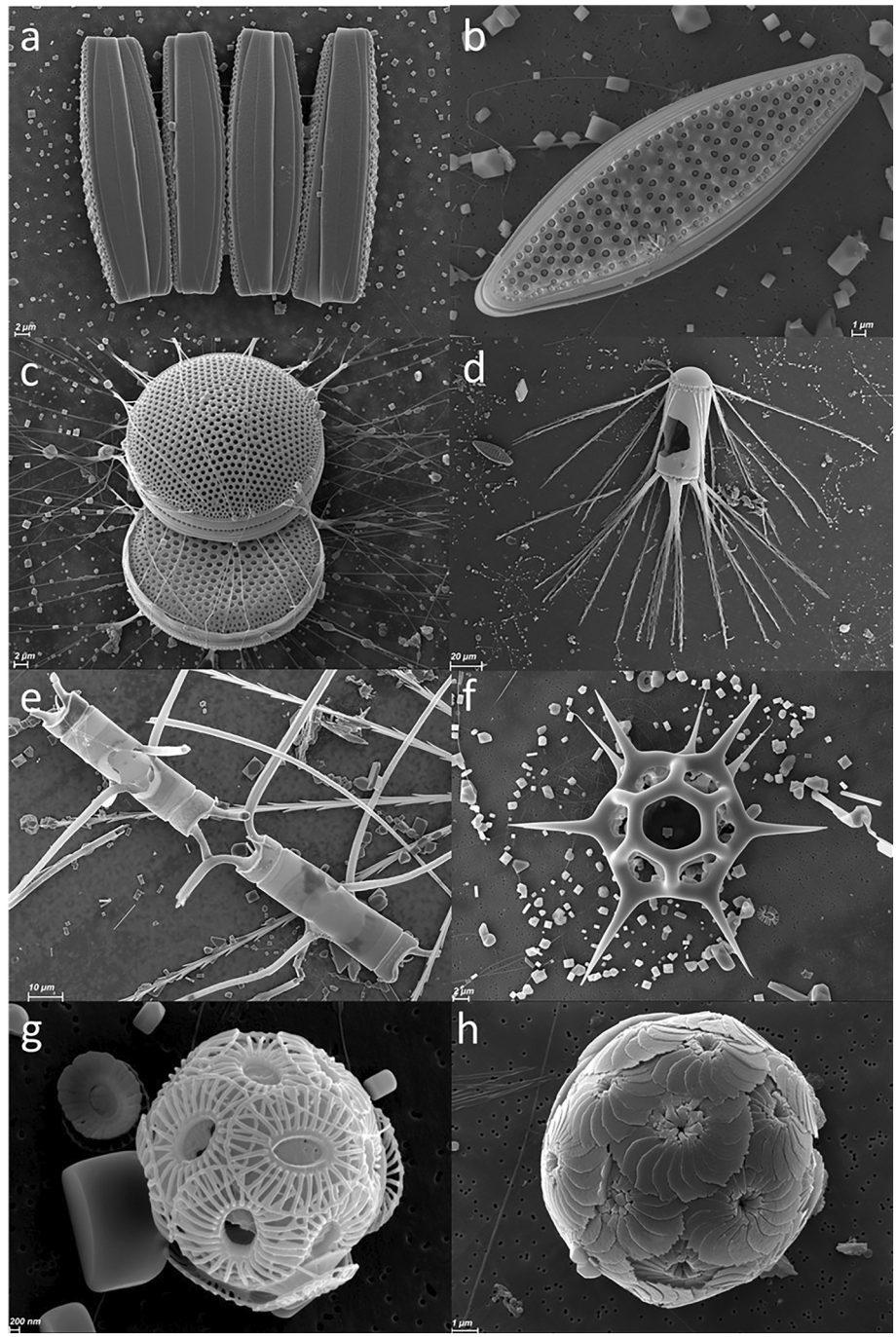

Figure 2. SEM images of phytoplankton sampled in the PFZ and the HNLC area, chain (a) and single cell (b) of Fragilariopsis kerguelensis (diatom) in HNLC area, (c) Thalassiosira sp. (diatom) in the PFZ, (d) Corethron sp. (diatom) in HNLC area, (e) Chaetoceros dichaeta (diatom) in HNLC area, (f) Stephanocha speculum (silicoflagellate) in HNLC area, (g) Emiliania huxleyi (coccolithophorid) and (h) Calcidiscus leptoporus (coccolithophorid) in the PFZ.

species, while nano- and pico-phytoplankton estimated by DP, accounted for 39% and 5% of the TChl *a*, respectively. Cell abundances from FCM was of 5.20 cells μL^{-1} (Table 2), exhibiting a lower abundance compared to the PFZ. Picophytoplankton represented 96% of the FCM phytoplankton abundance, while nano-phytoplankton accounted for approximately 4%. The concentrations of POC and PON closely mirrored those observed in the PFZ, with values of 4.99 and 0.74 µmol L^{-1}, respectively (Table 2). POC and PON concentrations were in the range of previous study in the HNLC domain (Tremblay et al., 2015).

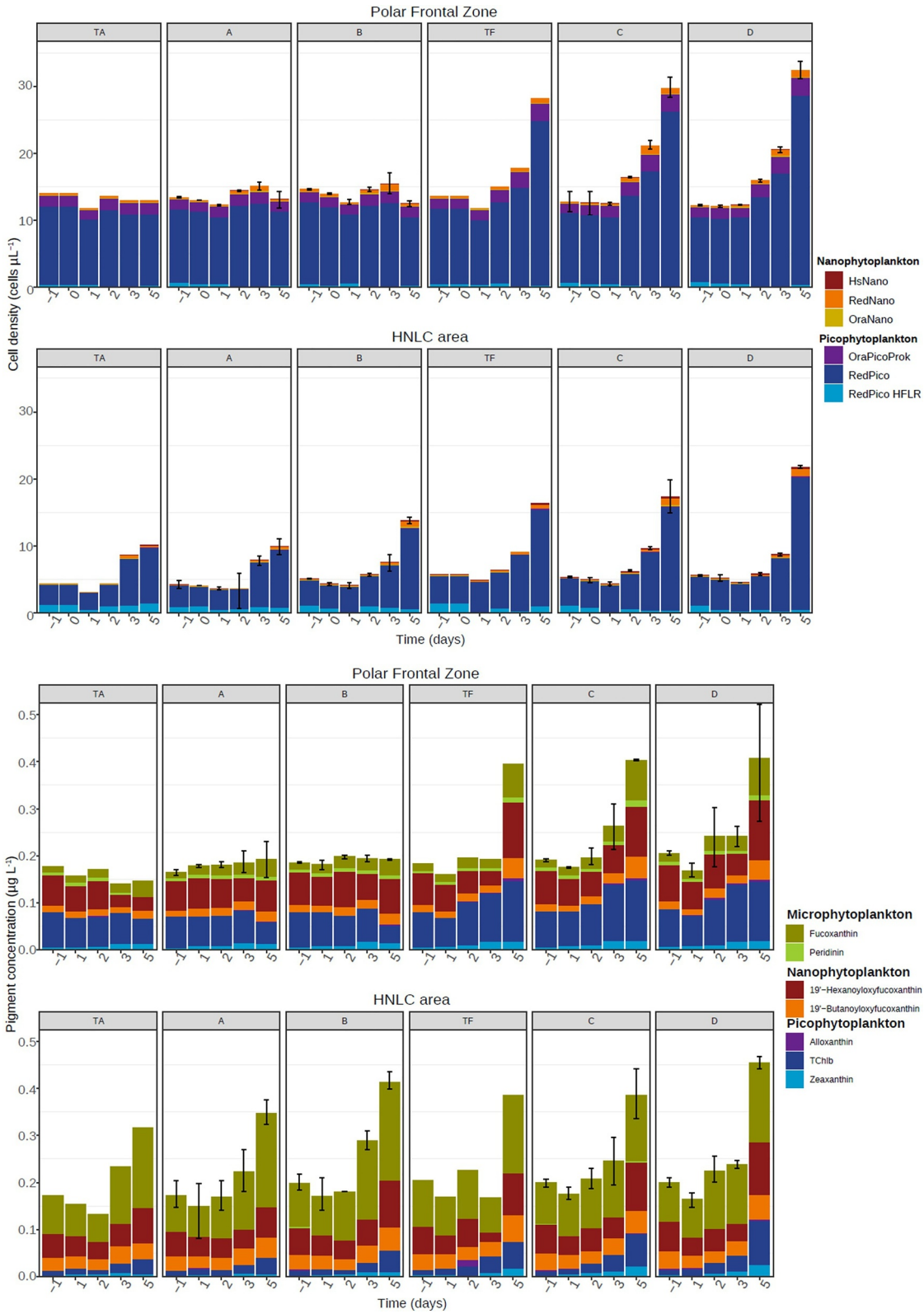
Polar Frontal Zone
TA
A
B
TF
C
D
Cell density (cells µL⁻¹)
HNLC area
Time (days)
Nanophytoplankton
HsNano
RedNano
OraNano
Picophytoplankton
OraPicoProk
RedPico
RedPico HFLR
Pigment concentration (µg L⁻¹)
Microphytoplankton
Fucoxanthin
Peridinin
Nanophytoplankton
19'−Hexanoyloxyfucoxanthin
19'−Butanoyloxyfucoxanthin
Picophytoplankton
Alloxanthin
TChlb
Zeaxanthin

Figure 3.

3.2. Impact on the Natural Phytoplankton Community

3.2.1. Polar Frontal Zone

The ANOVA test revealed a statistically significant difference in TChl *a* across the different scenarios and controls after 5 days (p-value = 0.02). After 2 days of incubation in +3°C and more acidic waters (scenarios C and D, and TF), both TChl *a* and total cell abundances began to increase significantly (p-value = 0.0008; Figures 3a and 3b). Conversely, under current *T* and pH conditions (scenarios A and B, and TA), a slight increase in biomass (p-value = 0.005) and slight decrease in cell abundance (p-value = 0.02) were observed after a 5-day incubation (Figures 3a and 3b). Furthermore, no significant difference was observed under the same *T* and pH conditions regardless of variations in dust additions (p-value = 1.00; Figures 3a and 3b). The contribution of diatoms (indicated by Fuco) increased more under future *T* and pH conditions (79% ± 4%, C and D) compared to current *T* and pH conditions (58% ± 5%, A and B). Similarly, the contribution of coccolithophorids (19'HF) and cyanobacteria (TChl *b* and Zea) also showed greater increases (38% ± 6%, 43% ± 4%, respectively). Within future scenario incubations and after 5 days, cell density rose by 50% in scenario TF (increase of 14.57 cells μL^{-1}), by ~57% in scenario C (+17.14 cells μL^{-1}) and by ~62% in scenario D (+20.34 cells μL^{-1}). Nanophytoplankton abundances exhibited no significant differences across all scenarios (p-value = 0.06), while picophytoplankton displayed substantial disparities (p-value = 0.01). Under warmer and acidification conditions, total cell density increased (p-value = 1.10^{-7}, scenarios TA, A, and B compared to TF, C, and D), particularly for nanophytoplankton (Figure 3a). However, despite this increase, picophytoplankton remained the dominant fraction of the phytoplankton in term of abundances, with no significant shifts recorded in the relative abundances of the pico- and nano-phytoplankton groups throughout the experiments.

3.2.2. HNLC Area

Over the 5 days incubation, TChl *a* concentration increased by 62%, 67%, 65%, 54%, 57%, and 66% for scenarios TA, A, B, TF, C, and D, respectively (Figure 3b), with a statistical difference among scenarios (p-value = 0.01). The increase in TChl *a* in the TA control can be due to water warming as the ship moved northward. The increase of TChl *a* concentration under current conditions with dust addition (scenarios A and B) was mainly due to an increase in diatom biomass (Fuco). Under the warmer and acidified conditions with dust addition (C and D), TChl *a* concentration increased significantly (p-value = 0.018) with higher dust added (*D*) (Figure 3), mainly driven by the increase of haptophytes (19'HF) and cyanobacteria (TChl *b* and Zea) (Figure 3). Total phytoplankton abundances estimated by FCM increased by ~65% in TA (+5.8 cells μL^{-1}), ~57% in A (+5.9 cells μL^{-1}), ~63% in B (+9.5 cells μL^{-1}), ~65% in TF (+10.6 cells μL^{-1}), ~68.8% in C (+12.3 cells μL^{-1}), and ~74% in *D* (+16.5 cells μL^{-1}) over the same period. The increase in nanophytoplankton cell abundance was stimulated by a doubling of dust input under future conditions (Figure 3a); however statistical analyses showed no significant differences in nanophytoplankton cell abundance across the tests (p-value = 0.17). In contrast, picophytoplankton cell abundance responded positively across all conditions (p-value = 0.03). Warming, acidification, and dust input notably promoted their growth more than dust addition alone (Figure 3), while nanophytoplankton cell abundance was comparably stimulated by dust addition under present (A, B) or future (C, D) conditions (Figure 3a). Despite environmental changes, no discernible shifts in the diatom assemblage were observed, with *F. kerguelensis* remaining dominant (Figures 2 and 3).

3.3. Impact on the Production of Particulate Organic Carbon

Patagonian dust contains lower levels of organic carbon and nitrogen compared to other types of atmospheric dusts that are more enriched, such as wildfire dust (Schlosser et al., 2017). This may explain why POC and PON

Figure 3. (a) Temporal evolution in cell density of phytoplankton groups in the PFZ and the HNLC area under distinct scenarios (TA, A, B, TF, C, and D). The t-1 value represents the sampling before dust addition and acclimatization to increase T and acidification, and t0 just after dust addition. RedPico refers to cyanobacteria, OraPicoProk to synechoccocus (cyanobacteria), HsNano to coccolithophorids and dinoflagellates, RedNano to cyanobacteria and cryptophytes, and OraNano to cyanobacteria, red algae and cryptophytes. Standard deviation was calculated using duplicates of the total number of cells. (b) Temporal evolution of phytoplankton pigment concentrations in the PFZ and the HNLC area under different scenarios (TA, A, B, TF, C, and D). Zeaxanthin and TChl b refers to cyanobacteria, Alloxanthin to cryptophytes, 19'-butanoyloxyfucoxanthin to haptophytes and pelagophytes, 19'-hexanoyloxyfucoxanthin to haptophytes, Peridinin to dinoflagellates, and fucoxanthin to diatoms based on the reference pigment classification (Uitz et al., 2006). The standard deviation was calculated using the duplicates of each scenario from the total Chl a.

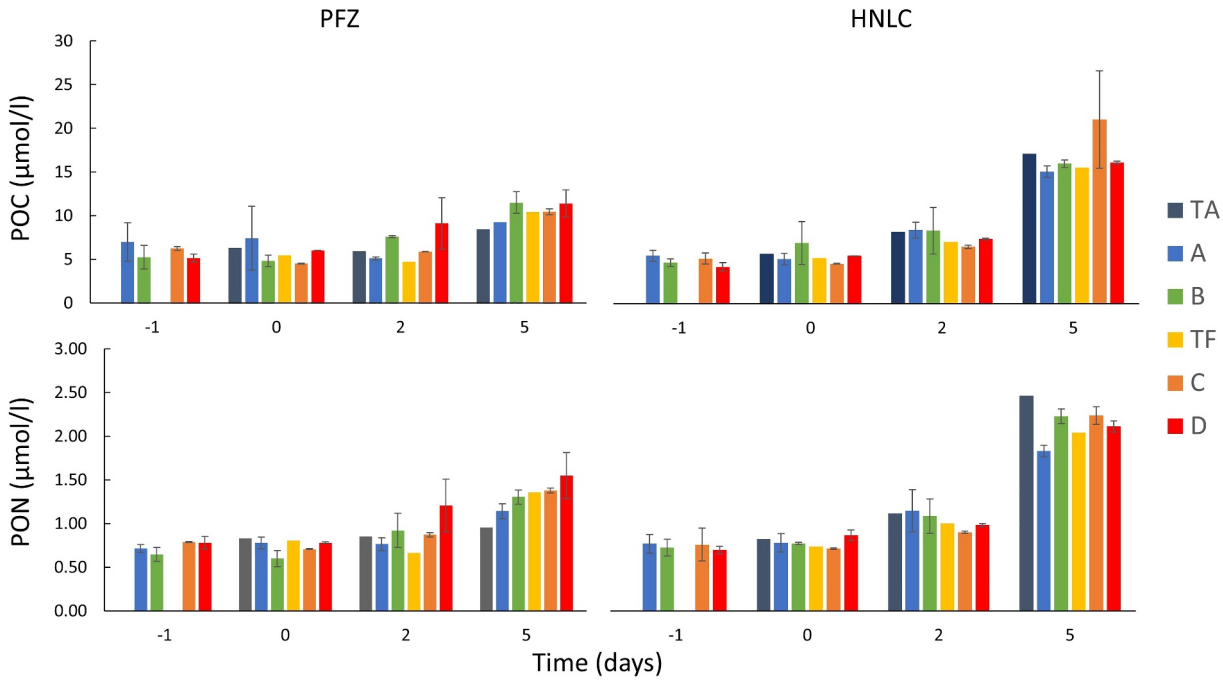

Figure 4. Evolution of particulate organic carbon (POC) and particulate organic nitrogen (PON) concentrations during the incubation with waters from the PFZ and the HNLC under different scenarios (TA, A, B, TF, C, and D). Standard deviation was determined from the average of duplicate experiments for each scenario.

concentration did not increase following dust deposition (Figure 4). The POC and PON concentrations in the incubations conducted with the PFZ waters nearly doubled after 5 days compared to their initial values, reaching ~10.8 µmol L^{-1} for POC and ~1.4 µmol L^{-1} for PON across all scenarios (Figure 4). In contrast, significantly higher increases were recorded in incubations using HNLC waters, with a threefold increase in POC (~15.8 µmol L^{-1}) and PON (~2.01 µmol L^{-1}) concentrations after 5 days of incubation (Figure 4). During 5 days, the net production rates of POC were estimated at 1.09 ± 0.26 µmol L^{-1} d^{-1} in the PFZ while higher rates of 2.07 ± 0.27 µmol L^{-1} d^{-1} were obtained in the HNLC area. A similar trend was observed in the production rate of PON, with 0.13 ± 0.03 µmol L^{-1} d^{-1} in the PFZ and 0.27 ± 0.04 µmol L^{-1} d^{-1} in HNLC area. However, no significant differences in POC and PON production were observed between the different scenarios within each zone.

The mean POC/PON ratio in the PFZ incubations (7.1 ± 0.7) was similar to that in the HNLC region (7.5 ± 0.9). Throughout the experimental period, the POC/PON ratio increased over the 5 days, reaching approximately 8.1 in the PFZ and 7.6 in the HNLC across all scenarios at the end of the experiments.

4. Discussion

4.1. Impacts in the Polar Frontal Zone

The phytoplankton abundance was typical of summer conditions, with surface waters in the PFZ commonly exhibiting abundances around ~13.4 ± 1.1 cells µL^{-1} (Fiala et al., 2003; Geisen et al., 2022). TChl *a* concentrations (0.18 ± 0.01 µg L^{-1}) in the Indian sector of the PFZ waters during the late summer were notably lower than those recorded in the Atlantic sector during spring (concentrations reaching up to 4.5 µg L^{-1}; Dafner & Mordasova, 1994; Whitehouse et al., 1996), which is consistent with the decrease of TChl *a* levels after the late spring or early summer bloom occurring in the PFZ (Weir et al., 2020; Xiuren et al., 1996). The presence of diatom species, including central diatoms and *Pseudonitzschia* sp., matched with known occurrences in the PFZ during summer (Rigual-Hernández et al., 2016; Shramik et al., 2013; Shukla et al., 2016; Smetacek et al., 2002). Furthermore, environmental changes lead to a decrease in the proportion of central diatoms, and an increase of the proportion of *Pseudonitzschia* species. In addition, the abundance of *Gymnodinium* sp. (dinoflagellate) observed was consistent with previous findings in non-Fe limited waters of the PFZ of the Australian sector (De Salas et al., 2011; Kopczynska et al., 2001).

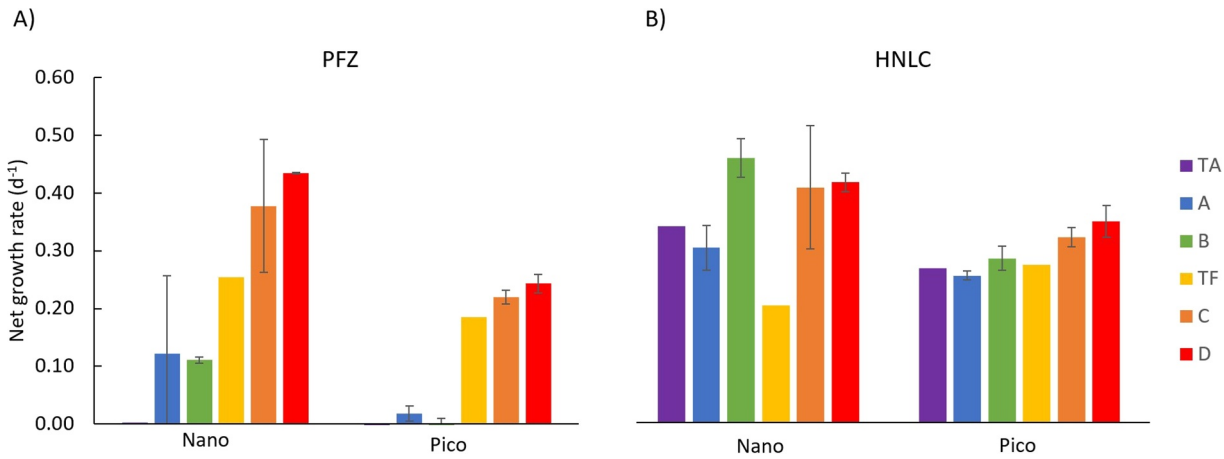

Figure 5. Net growth rate (estimated from abundance changes between initial and final incubation time) of nano- and pico-phytoplankton over a 5-days period under different scenarios (TA, A, B, TF, C, and D) in the PFZ and HNLC area. Standard deviation was determined from the average of the duplicate experiments for each scenario. For the PFZ, the "TA" bar does not appear as it was too close to 0.

Under the current conditions, the addition of dust alone did not stimulate the net growth of pico- and nano-phytoplankton (Figure 5), even if temperature decreased during the experiment. This lack of net growth stimulation in these smaller organisms in response to Fe-dust input suggested that they were likely not limited by dissolved Fe concentrations, which is consistent with previous findings in this region (Gilbert et al., 2022). Some species of cyanobacteria, including *Trichodesmium* sp., can assimilate particulate aerosol fractions (Polyviou et al., 2018; Sugie et al., 2013). In this study, the lack of response to dust addition observed in the PFZ also indicated that cyanobacteria were probably not limited by particulate Fe concentrations (6.96 ± 1.52 μmol L^{-1}, Table 2). On the other hand, the cooling of the waters when the ship was underway southwards could have slowed the growth, as many phytoplankton species, including cyanobacteria, which typically thrive in warmer conditions (Carey et al., 2012). This is consistent with the observed negative growth rate for cyanobacteria, although the rate remained relatively low. In contrast, the increase in microphytoplankton in TA could be linked to the cooling, which favors the growth of polar diatoms. The addition of Fe-dust alone also had no effect on the diatom biomass (Figure 3) as well as the nitrate concentration, which showed only a slight decrease at the end of the incubation compared to ambient water (from 19.4 ± 0.69 to 17.8 ± 0.71 μmol L^{-1}). In fact, diatoms were likely limited by the low silicate concentrations (~7.8 μmol L^{-1}) measured in these surface waters (Table 2), since Si-limitation of diatoms living in the PFZ region can typically occur at silicate levels below 20 μmol L^{-1}, which can be mainly due to the low affinity for Si uptake at Si concentrations ranging from 0.7 to 10 μmol L^{-1} (Nelson et al., 2001). Additionally, by the end of incubation, Si concentrations remained relatively stable across all scenarios (7.74 ± 0.43 μmol L^{-1}). The increase of POC and PON concentrations observed under the current conditions, whether dust was added or not (Figure 4) contrasted with the lack of increase in diatoms and smaller species (Figure 3). It suggested that photosynthesis was decoupled from the growth over 5 days (Leles & Levine, 2023; Morel, 1987; Schuback et al., 2015, 2017).

The anticipated environmental changes significantly boosted both cell density and biomass throughout the entire phytoplankton community (Figure 3). These changes notably favored the proliferation of the picophytoplankton which exhibited a net growth rate of 0.45 d^{-1} (Figure 5). Thus, the +3°C compared to ambient *T* and acidification of waters actually stimulated the growth of the nano- and pico-phytoplankton, as previously observed (Lin et al., 2012). For instance, coccolithophorids (nanophytoplankton, Figures 2g and 2h), evidenced by its contribution to TChl *a* (19'HF), that are prevalent along the Great Calcite Belt between the Subtropical Front and the Polar Front during the austral summer (Balch et al., 2011), increased in scenarios C and D. These algae may have benefited from acidification due to the increased availability of CO_2, which likely stimulated the functioning of the Rubisco enzyme (Winter et al., 2014), despite potential negative effects on their calcification (Zhang et al., 2020). Furthermore, diatom contribution increased under future conditions compared to present conditions (Figure 3), suggesting a positive cumulative impact of +3°C, acidification and increased Patagonian dust input on diatoms of the PFZ. Previous studies have also highlighted the beneficial effect of warming on a subantarctic diatom (Boyd et al., 2016) and the combined positive influence of warming and Fe on diatom species (Zhu

et al., 2016). Here, the rise in partial pressure of CO_2 under acidification could have played a key role, as diatoms exhibit a lower diffusive flux of CO_2 relative to their carbon demand (Wu et al., 2014). Diatoms could potentially benefit more from increased CO_2 partial pressure compared to coccolithophorids (Saini et al., 2021). Additionally, diatoms with silica frustules are less vulnerable to acidification than calcifying species (Meyer & Riebesell, 2015). Although the future conditions did not lead to significant shifts in the phytoplankton community, nanophytoplankton exhibited the most pronounced response to these changes, followed by picophytoplankton (Figures 3 and 5). The organic carbon content of nano- and pico-phytoplankton is generally lower than that of microphytoplankton (Edwards et al., 2012). As a result, the production of POC remained lower in the PFZ dominated by nano- and pico-phytoplankton (Figure 4). In polar areas, smaller species such as the cyanobacterium *Synechococcus* sp. contribute minimally to POC production (Buitenhuis et al., 2012), which may explain why the change in POC production between current and future conditions was similar.

4.2. Impacts in the HNLC Area

The nano- and pico-phytoplankton abundance observed in the ambient seawater (5.08 ± 0.61 cells μL^{-1}) was in the range of cell abundances previously documented in HNLC regions during austral summer (typically ranging from 0.001 to 10 cells μL^{-1}) (Lin et al., 2012). The prevalent contribution of diatoms (33%) to TChl *a* was also consistent with previous observations in this area (comprising approximately 20%–50% of the TChl *a*; Alvain et al., 2008).

The addition of dust under present *T* and pH conditions led to an increase in TChl *a* concentration (Figure 3), principally due to the increased contribution of diatoms (mainly *F. kerguelensis*), which already dominated in the ambient HNLC waters. Similar fertilization effects on diatoms following the addition of Patagonian or volcanic dust have been documented in these waters (Geisen et al., 2022), highlighting the Fe-limitation of diatoms in this HNLC area. In addition, Fe is one of the elements that dominate Patagonian dust (Demasy et al., 2024). Diatoms were observed either as single large cells or in small chains, as identified using the scanning electron microscope (Figure 2a). Chain-forming diatoms are produced by the fusion of siliceous tubular fibers, ensuring the solidity of the chain (Hildebrand et al., 2008; Mayzel et al., 2021; Nguyen & Fauci, 2014). Larger cells may experience greater Fe limitation than smaller cells due to their lower surface-to-volume ratio, resulting in higher constraint on Fe diffusion to the cell surface (Morel et al., 1991; Timmermans et al., 2001). Our results support this Fe-limitation observed in large and/or chain-forming Antarctic diatoms, which responded most positively to Fe-dust additions, likely facilitated by sufficient silicate concentration (27.50 µmol L^{-1}) in these waters, which remained stable in all scenarios during the incubation (27.20 ± 0.94 µmol L^{-1}). The high nitrate concentration in the ambient water (27.50 ± 0.89 µmol L^{-1}) decreased at the end of the experiment (24.13 ± 0.21 µmol L^{-1}) but remained at high concentration. The fertilization effect of diatoms resulting from Fe-dust input could also be attributed to their strong capacity to assimilate atmospheric dust through various biological mechanisms, such as direct absorption, enzymatic hydrolysis, mixotrophy and symbiotic relationship with the microbial community (Nygaard & Tobiesen, 1993; Reinl et al., 2022). Additionally, the size of diatoms (>20 µm) (Figure 2), superior to the dust (<10 µm), may potentially enhance the ability to phagocytose atmospheric elements, thereby enabling the direct uptake (Reinl et al., 2022). Furthermore, large-phytoplankton like *F. kerguelensis* have demonstrated the ability to directly use Fe bound to strong organic ligands (Strzepek et al., 2011) and to use Fe in colloidal forms (Hassler & Schoemann, 2009), which account for a significant portion of dissolved Fe in seawater of the SO and dust (Aguilar-Islas et al., 2010; Boye et al., 2010; Wells & Goldberg, 1993). Consistent with the Fe-fertilization effect on diatoms biomass due to Fe-dust input and the absence of Si-limitation in these waters, the production of POC by diatoms also increased under these conditions (0.27 ± 0.04 µmol L^{-1} d^{-1}).

Future environmental changes led to increased cell densities and diatom biomass, mainly due to the stimulation of nano- and pico-phytoplankton (Figure 3). Changes in temperature during transit were superimposed with treatment variations, potentially leading to over- or under-estimation of the observed responses. The warmer waters (+3°C) and northward sailing from colder to warmer waters might have benefited smaller species. In contrast, diatoms were at a disadvantage in the future *T* and pH conditions compared to dust addition alone under present conditions, although they still dominated the phytoplankton assemblage. Under future conditions, longer and more numerous chains of diatoms were formed (Figure 2a). The formation of diatom chains can enhance their gravitational sedimentation, facilitating vertical migrations (Lovecchio et al., 2019), and serve as a defense mechanism against zooplankton grazing, particularly for larger cells (Bjærke et al., 2015). However, grazing effects were not simulated in our study to prevent potential top-down regulation of phytoplankton responses to

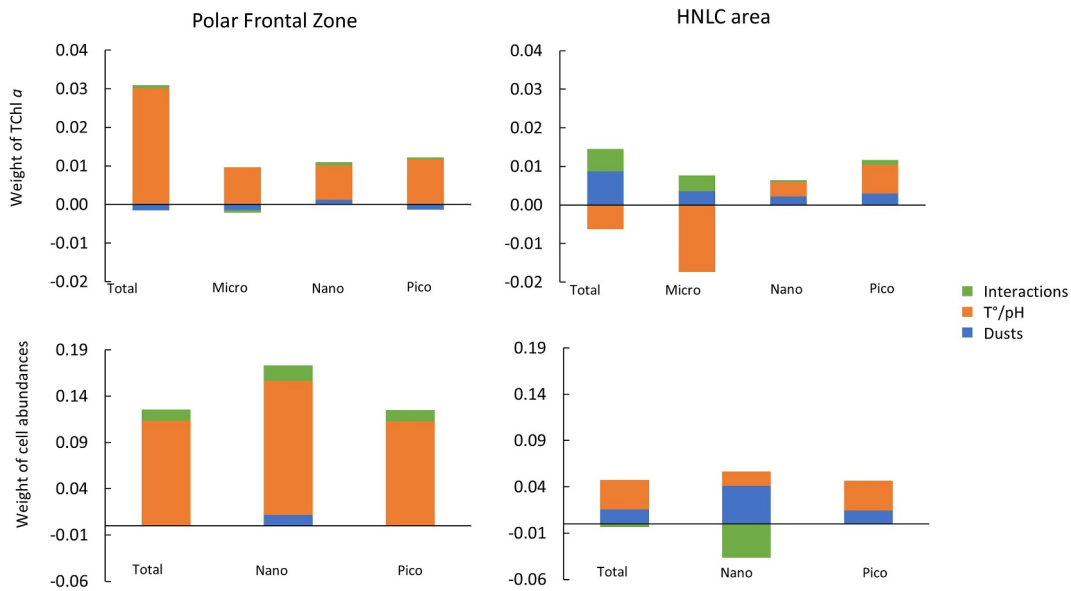

Figure 6. Individual versus interactive effects of dust input and other factors (warming and acidification) on the cell densities and biomasses. Total biomass was associated with TChl a, diatom biomass (microphytoplankton) with fucoxanthin, cyanobacteria (picophytoplankton) with zeaxanthin and total chlorophyll b, and haptophytes, like coccolithophorids (nanophytoplankton) with 19'-hexanoyloxyfucoxanthin. Total cell density was associated with growth rate of each size-cell abundance, cyanobacteria with OraPicoProk and RedPico, and nanophytoplankton with HsNano. The changes in biomass and cell density between day 5 and day 0 were used in the statistical model (Goupy, 1993).

environmental changes. Surprisingly, warming has been shown to have a stronger positive effect on the Antarctic diatom growth when supplemented with Fe (Raven & Geider, 1988). However, acidification, especially with high Fe input, can shift from neutral to negative effects for diatoms (Marchetti & Harrison, 2007). Acidification has been observed to counterbalance the positive impact of Fe input on a subantarctic diatom and mitigate the positive response of this diatom both to warming and Fe enrichment (Boyd et al., 2016; Trimborn, Brenneis, et al., 2017). Our findings are consistent with these observations, highlighting the antagonistic effect of acidification and warming on the intensification of Patagonian dust input on diatom biomass in the HNLC area. Despite these antagonist effects, the production of POC and PON was similar under future and present conditions (Figure 4), with concentration in the same range of the Redfield ratio (6.6) (Redfield, 1934) and consistent with typical POC/PON ratios observed in oceanic phytoplankton cells (5.0–13.3; Finkel et al., 2010). The similar production of POC and PON could be attributed to the fact that warming can reduce the cellular POC content in diatoms (Krause & Lomas, 2020), which may explain why, despite an increase in TChl *a* and cell numbers, the overall POC concentration remains unchanged. The consistency in POC and PON production may also be attributed to the insufficient changes in cell number and TChl *a* between scenarios. Instead, POC and PON production differences are likely more dependent on the specific species present (Basu & Mackey, 2018), which could explain the difference reported between the PFZ and the HNLC area. Indeed, the higher POC production in the HNLC area after 5 days of incubation compared to the PFZ might be attributed to larger *F. kerguelensis* cells in the HNLC area (Timmermans & Van Der Wagt, 2010), which store more POC than smaller diatoms and dinoflagellates (*Gymnodinium* sp.) observed in the PFZ (Kopczynska et al., 2001; Trimborn et al., 2013). Consequently, the anticipated future conditions might not lead to changes in POC production.

4.3. Weight of Environmental Changes on Phytoplankton Responses in the Two Biogeochemical Domains

A statistical model employing a 2^2 factorial design (Goupy, 1993) was used to estimate the weight of individual impacts of dust addition, +3°C compared to ambient *T* and acidification, as well as their interactions, on the cell density and the TChl *a* of the phytoplankton species (Figure 6). In the case where these different parameters trigger biological responses that diverge (stimulation or inhibition), the model may yield negative weights representing inhibition effects (Figure 6).

In the PFZ, +3°C and acidification were the main drivers of the increase TChl *a* and cell abundances (Figure 3), notably of the picophytoplankton that proliferated under future conditions (Figure 5). Conversely, in the HNLC area, dust input contributed significantly to the increase of TChl *a*, while +3°C and acidification were major contributors to the increase in abundances of smallest cells (Figure 6). The differing biological responses to environmental factors between these two biogeochemical domains predominantly stemmed from variations in diatom behavior. Specifically, in the PFZ, diatoms primarily responded to +3°C and acidification, whereas in the HNLC area, their response was influenced by Fe-dust input and the combined negative effects of acidification and warming (Figure 6). This disparity might be explained by fundamental differences in diatom species between the regions, with central diatoms and *Pseudonitzschia* sp. predominating in the PFZ, while *F. kerguelensis* was predominant in the HNLC region (Figure 2). Considering potential biases in future predictions when considering only individual impact of multiple stressors in experimental studies, our research strongly suggested divergent diatom responses to forthcoming changes in environmental conditions. While diatoms might thrive in response to +3°C and acidification in the PFZ (Figure 3) and the SAZ (Boyd et al., 2016), these changes could conversely negatively impact diatoms in the HNLC area (Figure 3). In this area, diatoms were primarily influenced by the positive effects of Fe, however, increasing the Fe input by twofold did not amplify this effect (Figure 6). This can be attributed to the fact that the anticipated doubling of dust input by 2,100 is unlikely to increase the Fe bioavailability in the HNLC area (Demasy et al., 2024).

The primary beneficiaries of future +3°C and acidification in surface waters across both biogeochemical domains were the nano- and pico-phytoplankton. Specifically, cyanobacteria (picophytoplankton) demonstrated a positive response primarily to warming and acidification in both zones (Figure 6). This response was consistent with the increased metabolism of cyanobacteria under warmer waters, where they thrive at temperatures above 25°C (Bender et al., 2014; Visser et al., 2016). Similarly, nanophytoplankton were stimulated by these environmental changes, with +3°C and acidification playing a key role (Figure 6), as previously observed (Trimborn, Thoms, et al., 2017). The adverse effects of dust input in the PFZ on micro- and pico-phytoplankton was difficult to explain, but they remained limited compared to the positive impact of +3°C and acidification. In the HNLC area, the observed detrimental impact on microphytoplankton due to warming and acidification can be attributed to the increased vulnerability of *F. kerguelensis* to environmental changes compared to other diatom species prevalent in the PFZ.

4.4. Expected Changes in Phytoplankton Species Composition and Primary Production in the Southern Ocean

The interactions among environmental factors are still unexplored and warrant special attention. Changes in temperature, light and pH can alter chemical forms, bound structures, interactions between chemical species, and the residence time of elements in seawater (Hutchins & Boyd, 2016), which in turn can subsequently alter the bioavailability of both micro- and macro-nutrients (Demasy et al., 2024). Numerous studies have shown opposing conclusions regarding chemical changes under future conditions. Moreover, phytoplankton may develop diverse adaptive strategies to cope with nutrient availability under the pressure of environmental changes (Basu et al., 2019), further complexifying the study of these interactions. Interpreting these experiments requires caution, as the small-scale nature of the onboard incubation and experimental closed system could not capture long-term ecological dynamics, such as adaptation and competition of species over decadal timescales. Additionally, the study did not consider oceanographic physical processes, including variations in the mixed layer depth and meso-to sub-mesoscale physical processes. However, while it is impossible to consider all factors, this study provided a controlled framework to investigate the interactions between physico-chemical environmental parameters across different phytoplankton groups.

Smaller algae, particularly cyanobacteria, which were prevalent in the PFZ during the austral summer, grew preferentially in future warmer waters, a trend observed in the PFZ and the HNLC area. Climate change projections support a potential increase in their geographical distributions and abundance as surface seawaters continue to warm (Flombaum et al., 2013). Likewise, haptophytes, especially coccolithophorids, benefited from warming of the waters in both domains. The increase in stratification within the SO since 1960 (Li et al., 2020) could particularly benefit coccolithophorids, which preferentially thrive in stratified waters (Brown & Yoder, 1994). Additionally, their proliferation may be enhanced by intensification of Fe-dust input (Boyd et al., 2016; Mahowald et al., 2010), as observed in our HNLC area incubations. Presently, the largest haptophyte blooms appear in regions impacted by Patagonian dust deposition in the southern Indian sector (Alvain

et al., 2008). Anticipated environmental changes could lead to an intensification of haptophyte blooms and a southward expansion of these species. Indeed, documented migration of coccolithophorids from northern to southern latitudes in the SO has been reported since last decades (Patil et al., 2017; Winter et al., 2014).

Albeit smaller species are a key cornerstone in the context of warming and acidification, diatoms play a crucial role in the SO, particularly for their role in the efficiency of the biological carbon pump. Diatoms in the PFZ, especially central diatoms and *Pseudonitzschia* sp. appeared to benefit more from +3°C and acidification compared to diatoms found in the HNLC area, such as *F. kerguelensis* (Figures 2 and 3). The response of diatoms in the PFZ possibly highlighted their ability to adapt to increasing seasonal warming associated with climate change. However, acidification may alter the nutritional value of Antarctic diatoms (Duncan et al., 2022). While Si-limitation could prevent diatoms from blooming in the future conditions in the PFZ (Deppeler & Davidson, 2017), acidification and warming could counteract the positive effect of increased Fe-dust input on diatoms in the HNLC area. Despite the enhanced Fe supply and possible positive effect of warming (Boyd et al., 2016), our finding suggested that diatoms may compete poorly with smaller phytoplankton species in potentially lower-Si waters in the PFZ.

Our study suggested that phytoplankton species composition in the future SO may not be altered, with the prevalence of nano- and pico-phytoplankton in the PFZ during late summer and of diatoms in the HNLC area. The projected production of POC was also expected to be similar to current levels in each domain, due to the stimulation of smaller species in the PFZ and to the negative impact of warming and acidification on the diatoms in the HNLC area. This suggested that primary production may not change in the future SO. However, the increase in number and length of chain-forming diatoms as observed under future conditions in the HNLC area may imply an intensification of POC export to deeper waters (Lovecchio et al., 2019; Mouw et al., 2016). Additionally, these chains are less prone to grazing by zooplankton (Bjærke et al., 2015). For instance, it has been reported that half of the biomass produced during a diatom bloom in the SO is exported to depths greater than 1,000 m through processes such as mucilaginous aggregates, cellular entanglements and chain formation (De La Rocha et al., 2008; Smetacek et al., 2012).

Our experimental findings suggested that pico- and nano-sized phytoplankton may preferentially increase in Si-limited waters under future conditions in PFZ, potentially enhancing the transfer efficiency of particulate matter through the upper trophic food-chain and microbial loop. However, our results do not align with predictions of increased net primary production (Kessler & Tjiputra, 2016). Models also predict an increased carbon export, primarily driven by phytoplankton responses to higher Fe inputs, shallower mixed layer, and warming across much of the SO (Henley et al., 2020). Correspondingly, models project increased carbon export in the SO by 21% in 2,100 under the RCP8.5 scenario (Sweetman et al., 2017). Yet, uncertainties persist regarding changes in phytoplankton growth rates and composition, the efficiency of the microbial loop, and its interaction with zooplankton (Henley et al., 2020).

Phytoplankton species have triggered a rapid response to projected in temperature, pH and dust input for 2,100 in our experimental study. However, phytoplankton are likely to undergo a longer adjustment period to adapt to changing environmental conditions over the next 80 years in the SO, which could result in distinct long-term responses. However, if the changes of conditions occur more gradual, phytoplankton could take advantage of the mosaic of environments favorable to its growth, potentially leading to a migration of populations from the north to the south concomitant with that of the fronts in the SO (Billany et al., 2010). Nevertheless, regardless of the direction of migration, nutrient availability will remain a critical factor shaping the future evolution of phytoplankton assemblages (Wyatt et al., 2023).

5. Conclusion

By the 2,100 horizon, projected environmental changes in the SO, including intensification of Patagonian dust input, warming, and acidification, are expected to elicit diverse responses among phytoplankton species inhabiting both the waters of the PFZ and HNLC (Figure 7). This study is the first to simulate the combined impact of Patagonian dust, a +3°C temperature increase, and acidification on the natural phytoplankton communities from the PFZ and HNLC area of the SO.

Our experimental study showed that different phytoplankton responses to these future environmental changes in the two distinct biogeochemical regimes of the PFZ and HNLC area (Figure 7). Indeed, small phytoplankton

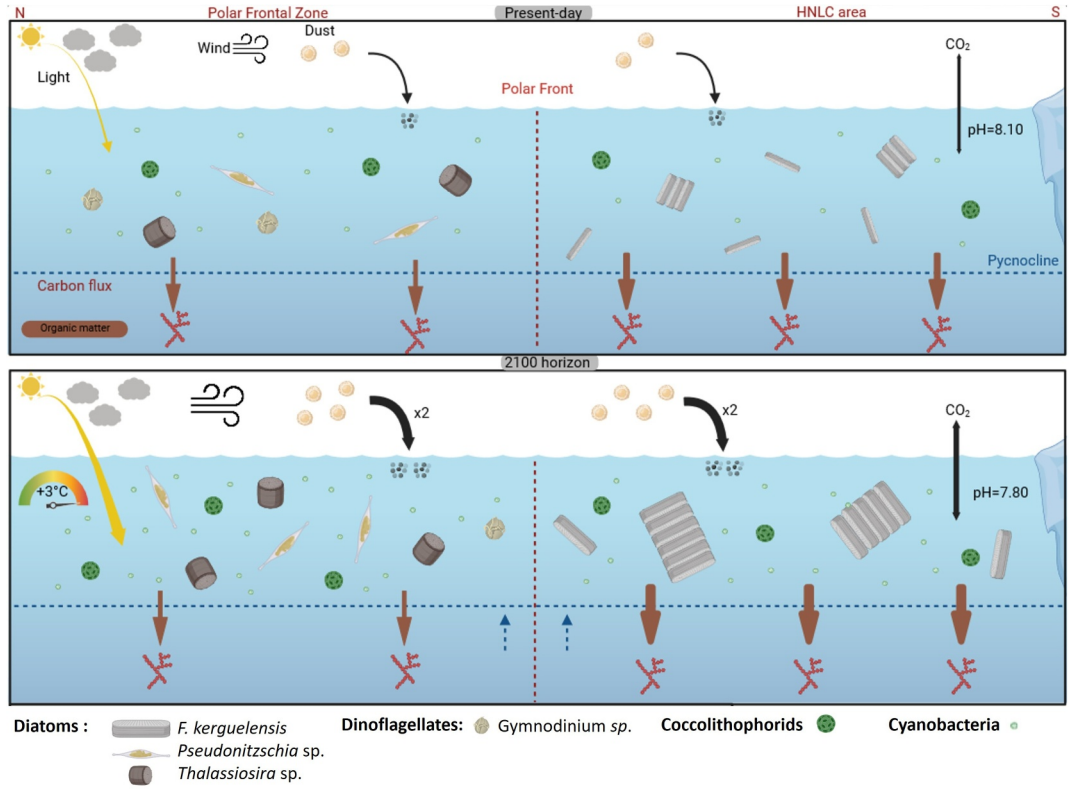

Figure 7. Conceptual schematic illustrating the present conditions (top panel) and the anticipated environmental change (lower panel) and their interactive effects on phytoplankton in the Polar Frontal Zone (left) and the HNLC area (right) of the Southern Ocean. This visual was generated using BioRender website.

species may benefit most from future temperature increases in the PFZ, while increased Fe-inputs would not have a significant impact on the phytoplankton in this region during the austral summer. Future environmental changes may not alter the composition of the phytoplankton assemblage in the PFZ, nor the primary production. Conversely, future intensification of Fe-dust input in the HNLC zone may strongly benefit to larger phytoplankton, especially diatoms. However, this Fe-fertilization effect may be counteracted by the negative impact of future acidification and warming on diatoms. Nevertheless, the composition of the phytoplankton assemblage dominated by large diatoms and the primary production may not be altered by the future environmental changes in the HNLC area. However, the increase in the number and length of diatom chains could lead to an increase in export of particulate organic carbon in the future HNLC domain.

To comprehensively understand the implications of environmental changes and dust input in the SO ecosystem, additional research is needed. For instance, longer-term experiments (>5 days) could better elucidate the evolution of phytoplankton assemblages and its adaptation to long-term changes in the environmental conditions. While the study identified distinct biogeochemical responses depending on the domain studied, seasonality plays also a crucial role, especially in the PFZ. Changes in environmental conditions may influence phytoplankton communities in varying ways, particularly before the summer bloom, when nutrient concentrations can undergo drastic changes. Given the role of zooplankton predation on phytoplankton, exploring its impact on phytoplankton could help uncover cascading effects within the upper trophic chain. Additionally, heterotrophic prokaryote activity deserves particular attention since it significantly impacts the exported flux of organic matter at depth. Assessing interactions between the different micro-organisms of the trophic chain could highlight the potential positive or negative effects of environmental changes on the future trajectory of the biological carbon pump in the SO. In summary, this work has enabled the exploration of environmental co-impacts, which current models often fail to capture due to their limitations. Many models assume that factors act independently, overlooking their complex interactions, which are not always linear and may involve spurious relationships. By addressing these

gaps, this study has contributed to a deeper understanding of these interactions and their environmental implications.

Data Availability Statement

The original data presented in this manuscript were acquired as part of the SO-dust project funded by the LEFE-CYBER program of the French INSU-CNRS (Demasy et al., 2025). *Softwares*: The figures were produced using ggplot2 package (Wickham et al., 2007). The visual in Figure 7 was generated using BioRender website. The raw data generated by the CytoSense flow cytometer using the CytoUSB control software underwent processing using CytoClus 4 software (Demasy et al., 2025). ANOVA tests (Fisher, 1992) supplemented by a Tukey test (Tukey, 1949) were performed using rstatix package (Kassambara, 2019) to analyze significant differences in cell density (flow cytometry) and pigments (HPLC) between the scenarios. The relative weight of selected stressors (dust addition, and the combination of pH and temperature) and their interactions on changes in abundances of phytoplankton flow cytometry groups and pigment concentrations were estimated using statistical model employing a 2^2 factorial design (Goupy, 1993). *Databases*: Phytoplankton were identified to the lowest taxonomic level achievable (species, genus or group) using classical manuals for marine phytoplankton identification (In Scott & Marchant, 2005; Tomas, 1997) and the World Register of Marine Species database (WoRMS Editorial Board, 2023). Post-processing of the cytograms yielded results that quantified the abundance of distinct phytoplankton groups (Malkassian et al., 2011; Thyssen et al., 2022). The phytoplankton groups were classified and standardized according to the reference database F02 of Marine Microbial Flow Cytometry Standardised Group Names. Quantitative computations to determine total Chl *a* (TChl *a*) for each phytoplankton groups used the diagnostic pigments (Gieskes et al., 1988; Uitz et al., 2010).

Acknowledgments
This work was financially supported by the SO-dust project (Responses of phytoplankton to Patagonian dust input and anthropogenic changes in the future Southern Ocean, PI M. Boye) funded by the LEFE-CYBER program of the French INSU-CNRS. The SEM analyses were carried out within the high-resolution analysis platform (PARI) of the IPGP. The experiments were conducted on board the French *R.V. Marion Dufresne II* and we extend our special thanks to the Captain and the crew members for their assistance at sea and to the French National Observation Service in the Indian Ocean (SNO OISO) of INSU-CNRS led by Dr Claire Lo Monaco (LOCEAN, Paris) for joining their oceanographic campaign. We thank Dr Julia Uitz and Céline Dimier (Institut de la Mer de Villefranche, France) for the analyses of the phytoplankton pigment concentrations using HPLC within the National Analytical Platform SAPIGH of INSU-CNRS. We acknowledge Béatriz Beker for the taxonomic analyses of phytoplankton. We also extend special thanks to the French MAP-IO program (Marion Dufresne Atmospheric Program-Indian Ocean) coordinated by Dr Pierre Tulet (LACy, France) for the support in a flow cytometer onboard the ship. Thanks also to Emma Moreau (IPGP, Paris) for her help in data processing and to Prof Rémi Losno (IPGP, Paris) for providing the Patagonian soil.

References

Ackert, R. P., Jr. (2009). Patagonian dust machine. *Nature Geoscience*, *2*, 244–245. https://doi.org/10.1038/ngeo485

Aguilar-Islas, A. M., Wu, J., Rember, R., Johansen, A. M., & Shank, L. M. (2010). Dissolution of aerosol-derived iron in seawater: Leach solution chemistry, aerosol type, and colloidal iron fraction. *Marine Chemistry*, *120*(1–4), 25–33. https://doi.org/10.1016/j.marchem.2009.01.011

Alvain, S., Moulin, C., Dandonneau, Y., & Loisel, H. (2008). Seasonal distribution and succession of dominant phytoplankton groups in the global ocean: A satellite view. *Global Biogeochemical Cycles*, *22*(3). https://doi.org/10.1029/2007GB003154

Antajan, E., Chrétiennot-Dinet, M.-J., Leblanc, C., Daro, M.-H., & Lancelot, C. (2004). 19′-hexanoyloxyfucoxanthin may not be the appropriate pigment to trace occurrence and fate of *Phaeocystis*: The case of *P. globosa* in Belgian coastal waters. *Journal of Sea Research*, *52*, 165–177. https://doi.org/10.1016/j.seares.2004.02.003

Armand, L. K., Cornet-Barthaux, V., Mosseri, J., & Quéguiner, B. (2008). Late summer diatom biomass and community structure on and around the naturally Iron-Fertilised Kerguelen Plateau in the Southern Ocean. *Deep Sea Research Part II: Topical Studies in Oceanography*, *55*(5–7), 653–676. https://doi.org/10.1016/j.dsr2.2007.12.031

Arrigo, K. R., Mills, M. M., Kropuenske, L. R., Van Dijken, G. L., Alderkamp, A.-C., & Robinson, D. H. (2010). Photophysiology in two major Southern Ocean phytoplankton taxa: Photosynthesis and growth of *Phaeocystis antarctica* and *Fragilariopsis cylindrus* under different irradiance levels. *Integrative and Comparative Biology*, *50*(6), 950–966. https://doi.org/10.1093/icb/icq021

Attiya, A. A., & Jones, B. G. (2022). An extensive dust storm impact on air quality on 22 November 2018 in Sydney, Australia, using satellite remote sensing and ground data. *Environmental Monitoring and Assessment*, *194*(6), 432. https://doi.org/10.1007/s10661-022-10080-1

Balch, W. M., Drapeau, D. T., Bowler, B. C., Lyczskowski, E., Booth, E. S., & Alley, D. (2011). The contribution of coccolithophores to the optical and inorganic carbon budgets during the Southern Ocean Gas Exchange Experiment: New evidence in support of the "Great Calcite Belt" hypothesis. *Journal of Geophysical Research*, *116*, C00F06. https://doi.org/10.1029/2011JC006941

Barnes, D. K. A., Fuentes, V., Clarke, A., Schloss, I. R., & Wallace, M. I. (2006). Spatial and temporal variation in shallow seawater temperatures around Antarctica. *Deep Sea Research Part II: Topical Studies in Oceanography*, *53*(8–10), 853–865. https://doi.org/10.1016/j.dsr2.2006.03.008

Basu, S., Gledhill, M., de Beer, D., Prabhu Matondkar, S. G., & Shaked, Y. (2019). Colonies of marine cyanobacteria *Trichodesmium* interact with associated bacteria to acquire iron from dust. *Communications Biology*, *2*(1), 284. https://doi.org/10.1038/s42003-019-0534-z

Basu, S., & Mackey, K. (2018). Phytoplankton as key mediators of the biological carbon pump: Their responses to a changing climate. *Sustainability (Basel)*, *10*(3), 869. https://doi.org/10.3390/su10030869

Bender, D., Diaz-Pulido, G., & Dove, S. (2014). Warming and acidification promote cyanobacterial dominance in turf algal assemblages. *Marine Ecology Progress Series*, *517*, 271–284. https://doi.org/10.3354/meps11037

Billany, W., Swart, S., Hermes, J., & Reason, C. J. C. (2010). Variability of the Southern Ocean fronts at the Greenwich Meridian. *Journal of Marine Systems*, *82*(4), 304–310. https://doi.org/10.1016/j.jmarsys.2010.06.005

Bjærke, O., Jonsson, P. R., Alam, A., & Selander, E. (2015). Is Chain length in phytoplankton regulated to evade predation? *Journal of Plankton Research*, *37*, 1110–1119. https://doi.org/10.1093/plankt/fbv076

Boyd, P., Collins, S., Dupont, S., Fabricius, K., Gattuso, J.-P., Havenhand, J., et al. (2019). SCOR WG149 handbook to support the SCOR best Practice Guide for "multiple drivers" marine research. *University of Tasmania, on behalf of Scientific Committee on Oceanic Research (SCOR)*. https://doi.org/10.25959/5C92FDF0D3C7A

Boyd, P. W., Arrigo, K. R., Ardyna, M., Halfter, S., Huckstadt, L., Kuhn, A. M., et al. (2024). The role of biota in the Southern Ocean carbon cycle. *Nature Reviews Earth & Environment*, *5*, 390–408. https://doi.org/10.1038/s43017-024-00531-3

Boyd, P. W., Dillingham, P. W., McGraw, C. M., Armstrong, E. A., Cornwall, C. E., Feng, Y.-y., et al. (2016). Physiological responses of a Southern Ocean diatom to complex future ocean conditions. *Nature Climate Change*, *6*(2), 207–213. https://doi.org/10.1038/nclimate2811

Boye, M., Nishioka, J., Croot, P., Laan, P., Timmermans, K. R., Strass, V. H., et al. (2010). Significant portion of dissolved organic Fe complexes in fact is Fe colloids. *Marine Chemistry*, *122*(1–4), 20–27. https://doi.org/10.1016/j.marchem.2010.09.001

Bronselaer, B., Russell, J. L., Winton, M., Williams, N. L., Key, R. M., Dunne, J. P., et al. (2020). Importance of wind and meltwater for observed chemical and physical changes in the Southern Ocean. *Nature Geoscience*, *13*(1), 35–42. https://doi.org/10.1038/s41561-019-0502-8

Brown, C. W., & Yoder, J. A. (1994). Coccolithophorid blooms in the global ocean. *Journal of Geophysical Research*, *99*(C4), 7467–7482. https://doi.org/10.1029/93JC02156

Browning, T. J., Achterberg, E. P., Engel, A., & Mawji, E. (2021). Manganese co-limitation of phytoplankton growth and major nutrient drawdown in the Southern Ocean. *Nature Communications*, *12*(1), 884. https://doi.org/10.1038/s41467-021-21122-6

Browning, T. J., & Moore, C. M. (2023). Global analysis of ocean phytoplankton nutrient limitation reveals high prevalence of co-limitation. *Nature Communications*, *14*(1), 5014. https://doi.org/10.1038/s41467-023-40774-0

Bryłka, K., Alverson, A. J., Pickering, R. A., Richoz, S., & Conley, D. J. (2023). Uncertainties surrounding the oldest fossil record of diatoms. *Scientific Reports*, *13*(1), 8047. https://doi.org/10.1038/s41598-023-35078-8

Buitenhuis, E. T., Li, W. K. W., Vaulot, D., Lomas, M. W., Landry, M. R., Partensky, F., et al. (2012). Picophytoplankton biomass distribution in the global ocean. *Earth System Science Data*, *4*(1), 37–46. https://doi.org/10.5194/essd-4-37-2012

Carey, C. C., Ibelings, B. W., Hoffmann, E. P., Hamilton, D. P., & Brookes, J. D. (2012). Eco-physiological adaptations that favour freshwater cyanobacteria in a changing climate. *Water Research*, *46*(5), 1394–1407. https://doi.org/10.1016/j.watres.2011.12.016

Chapman, W. L., & Walsh, J. E. (2007). A synthesis of Antarctic temperatures. *Journal of Climate*, *20*(16), 4096–4117. https://doi.org/10.1175/JCLI4236.1

Coello-Camba, A., & Agustí, S. (2017). Thermal thresholds of phytoplankton growth in polar waters and their consequences for a warming polar ocean. *Frontiers in Marine Science*, *4*, 168. https://doi.org/10.3389/fmars.2017.00168

Constable, A. J., Melbourne-Thomas, J., Corney, S. P., Arrigo, K. R., Barbraud, C., Barnes, D. K. A., et al. (2014). Climate change and Southern Ocean ecosystems I: How changes in physical habitats directly affect marine biota. *Global Change Biology*, *20*, 3004–3025. https://doi.org/10.1111/gcb.12623

Dafner, E. V., & Mordasova, N. V. (1994). Influence of biotic factors on the hydrochemical structure of surface water in the Polar Frontal Zone of the Atlantic Antarctic. *Marine Chemistry*, *45*(1–2), 137–148. https://doi.org/10.1016/0304-4203(94)90098-1

De La Rocha, C. L., Nowald, N., & Passow, U. (2008). Interactions between diatom aggregates, minerals, particulate organic carbon, and dissolved organic matter: Further implications for the ballast hypothesis. *Global Biogeochemical Cycles*, *22*(4). https://doi.org/10.1029/2007GB003156

Demasy, C. (2023). *Solubility and bioavailability of Patagonian dust in the future Southern Ocean*. (PhD Thesis). Université Paris Cité.

Demasy, C., Boye, M., Delisée, A., Maguer, J.-F., Thyssen, M., & Gest, L. (2025). Phytoplankton incubations under Patagonian dust input and environmental changes in the Southern Ocean [Dataset]. *SEANOE*. https://doi.org/10.17882/105487

Demasy, C., Boye, M., Lai, B., Burckel, P., Feng, Y., Losno, R., et al. (2024). Iron dissolution from Patagonian dust in the Southern Ocean: Under present and future conditions. *Frontiers in Marine Science*, *11*, 1363088. https://doi.org/10.3389/fmars.2024.1363088

Deppeler, S. L., & Davidson, A. T. (2017). Southern Ocean phytoplankton in a changing climate. *Frontiers in Marine Science*, *4*. https://doi.org/10.3389/fmars.2017.00040

De Salas, M. F., Eriksen, R., Davidson, A. T., & Wright, S. W. (2011). Protistan communities in the Australian sector of the sub-Antarctic zone during SAZ-Sense. *Deep Sea Research Part II: Topical Studies in Oceanography*, *58*(21–22), 2135–2149. https://doi.org/10.1016/j.dsr2.2011.05.032

Ducklow, H., Steinberg, D., & Buesseler, K. (2001). Upper Ocean carbon export and the biological pump. *Oceanography*, *14*(4), 50–58. https://doi.org/10.5670/oceanog.2001.06

Duncan, R. J., Nielsen, D. A., Sheehan, C. E., Deppeler, S., Hancock, A. M., Schulz, K. G., et al. (2022). Ocean acidification alters the nutritional value of Antarctic diatoms. *New Phytologist*, *233*(4), 1813–1827. https://doi.org/10.1111/nph.17868

Dussart, B. (1992). Limnologie: L'étude des eaux continentales. In *Collection "Faunes et flores actuelles."* (2. éd). Boubée.

Edwards, K. F., Thomas, M. K., Klausmeier, C. A., & Litchman, E. (2012). Allometric scaling and taxonomic variation in nutrient utilization traits and maximum growth rate of phytoplankton. *Limnology & Oceanography*, *57*(2), 554–566. https://doi.org/10.4319/lo.2012.57.2.0554

Fiala, M., Delille, B., Dubreuil, C., Kopczynska, E., Leblanc, K., Morvan, J., et al. (2003). Mesoscale surface distribution of biogeochemical characteristics in the Crozet Basin frontal zones (South Indian Ocean). *Marine Ecology Progress Series*, *249*, 1–14. https://doi.org/10.3354/meps249001

Fiala, M., Kopczynska, E. E., Oriol, L., & Machado, M.-C. (2004). Phytoplankton variability in the Crozet Basin frontal zone (Southwest Indian Ocean) during austral summer. *Journal of Marine Systems*, *50*(3–4), 243–261. https://doi.org/10.1016/j.jmarsys.2004.01.008

Finkel, Z. V., Beardall, J., Flynn, K. J., Quigg, A., Rees, T. A. V., & Raven, J. A. (2010). Phytoplankton in a changing world: Cell size and elemental stoichiometry. *Journal of Plankton Research*, *32*(1), 119–137. https://doi.org/10.1093/plankt/fbp098

Fisher, R. A. (1992). Statistical methods for research workers. In S. Kotz & N. L. Johnson (Eds.), *Breakthroughs in statistics* (pp. 66–70). Springer Series in Statistics. Springer. https://doi.org/10.1007/978-1-4612-4380-9_6

Flombaum, P., Gallegos, J. L., Gordillo, R. A., Rincón, J., Zabala, L. L., Jiao, N., et al. (2013). Present and future global distributions of the marine Cyanobacteria *Prochlorococcus* and *Synechococcus*. *Proceedings of the National Academy of Sciences*, *110*(24), 9824–9829. https://doi.org/10.1073/pnas.1307701110

Franck, V. M., Brzezinski, M. A., Coale, K. H., & Nelson, D. M. (2000). Iron and silicic acid concentrations regulate Si uptake north and south of the Polar Frontal Zone in the Pacific Sector of the Southern Ocean. *Deep Sea Research Part II: Topical Studies in Oceanography*, *47*, 3315–3338. https://doi.org/10.1016/S0967-0645(00)00070-9

Gassó, S., & Stein, A. F. (2007). Does dust from Patagonia reach the sub-Antarctic Atlantic ocean? *Geophysical Research Letters*, *34*(1), L01801. https://doi.org/10.1029/2006GL027693

Geisen, C., Ridame, C., Journet, E., Delmelle, P., Marie, D., Lo Monaco, C., et al. (2022). Phytoplanktonic response to simulated volcanic and desert dust deposition events in the South Indian and Southern Oceans. *Limnology & Oceanography*, *67*(7), 1537–1553. https://doi.org/10.1002/lno.12100

Gieskes, W. W. C., Kraay, G. W., Nontji, A., Setiapermana, D., & Sutomo (1988). Monsoonal alternation of a mixed and a layered structure in the phytoplankton of the euphotic zone of the Banda sea (Indonesia): A mathematical analysis of algal pigment fingerprints. *Netherlands Journal of Sea Research*, *22*(2), 123–137. https://doi.org/10.1016/0077-7579(88)90016-6

Gilbert, N. E., LeCleir, G. R., Strzepek, R. F., Ellwood, M. J., Twining, B. S., Roux, S., et al. (2022). Bioavailable iron titrations reveal oceanic *Synechococcus* ecotypes optimized for different iron availabilities. *ISME Commun*, *2*(1), 54. https://doi.org/10.1038/s43705-022-00132-5

Gili, S., Vanderstraeten, A., Chaput, A., King, J., Gaiero, D. M., Delmonte, B., et al. (2022). South African dust contribution to the high southern latitudes and East Antarctica during interglacial stages. *Communications Earth & Environment*, *3*(1), 129. https://doi.org/10.1038/s43247-022-00464-z

Glibert, P. M., Song, Y., Zhang, F., Beusen, A. H. W., Bouwman, A. F., Burkholder, J. M., et al. (2020). 12 Multifaceted climatic change and nutrient effects on harmful algae require multifaceted models. In L. M. Botana, M. C. Louzao, & N. Vilarino (Eds.), *Climate change and marine and freshwater Toxins* (pp. 473–518). De Gruyter. https://doi.org/10.1515/9783110625738-012

Goupy, J. (1993). *Methods for experimental design: Principles and applications for physicists and chemists, data handling in science and technology*. Elsevier.

Hasle, G. (1988). The inverted-microscope method. In A. Sournia (Ed.), *Phytoplankton manual*. UNESCO.

Hassler, C. S., & Schoemann, V. (2009). Bioavailability of organically bound Fe to model phytoplankton of the Southern Ocean. *Biogeosciences*, *6*(10), 2281–2296. https://doi.org/10.5194/bg-6-2281-2009

Hauck, J., Völker, C., Wolf-Gladrow, D. A., Laufkötter, C., Vogt, M., Aumont, O., et al. (2015). On the Southern Ocean CO_2 uptake and the role of the biological carbon pump in the 21st century. *Global Biogeochemical Cycles*, *29*, 1451–1470. https://doi.org/10.1002/2015GB005140

Heimburger, A., Losno, R., Triquet, S., & Nguyen, E. B. (2013). Atmospheric deposition fluxes of 26 elements over the southern Indian ocean: Time series on Kerguelen and Crozet Islands. *Global Biogeochemical Cycles*, *27*(2), 440–449. https://doi.org/10.1002/gbc.20043

Henley, S. F., Cavan, E. L., Fawcett, S. E., Kerr, R., Monteiro, T., Sherrell, R. M., et al. (2020). Changing biogeochemistry of the Southern Ocean and its ecosystem implications. *Frontiers in Marine Science*, *7*, 581. https://doi.org/10.3389/fmars.2020.00581

Hildebrand, M., Doktycz, M. J., & Allison, D. P. (2008). Application of AFM in understanding Biomineral formation in diatoms. *Pfluegers Archiv European Journal of Physiology*, *456*(1), 127–137. https://doi.org/10.1007/s00424-007-0388-y

Hillebrand, H., Dürselen, C., Kirschtel, D., Pollingher, U., & Zohary, T. (1999). Biovolume calculation for pelagic and benthic microalgae. *Journal of Phycology*, *35*, 403–424. https://doi.org/10.1046/j.1529-8817.1999.3520403.x

Hutchins, D. A., & Boyd, P. W. (2016). Marine phytoplankton and the changing ocean iron cycle. *Nature Climate Change*, *6*(12), 1072–1079. https://doi.org/10.1038/nclimate3147

Jickells, T. D., An, Z. S., Andersen, K. K., Baker, A. R., Bergametti, G., Brooks, N., et al. (2005). Global iron connections between desert dust, ocean biogeochemistry, and climate. *Science*, *308*(5718), 67–71. https://doi.org/10.1126/science.1105959

Kassambara, A. (2019). Rstatix: Pipe-Friendly framework for basic statistical tests [Software]. *CRAN: Contributed Packages*. https://doi.org/10.32614/CRAN.package.rstatix

Kessler, A., & Tjiputra, J. (2016). The Southern Ocean as a constraint to reduce uncertainty in future ocean carbon sinks. *Earth System Dynamics.*, *7*(2), 295–312. https://doi.org/10.5194/esd-7-295-2016

Kopczynska, E. E., Dehairs, F., Elskens, M., & Wright, S. (2001). Phytoplankton and microzooplankton variability between the Subtropical and Polar Fronts south of Australia: Thriving under regenerative and new production in late summer. *Journal of Geophysical Research*, *106*(C12), 31597–31609. https://doi.org/10.1029/2000JC000278

Krause, J. W., & Lomas, M. W. (2020). Understanding diatoms' past and future biogeochemical role in high-latitude seas. *Geophysical Research Letters*, *47*(1). https://doi.org/10.1029/2019GL085602

Leber, G. M., Beal, L. M., & Elipot, S. (2017). Wind and current forcing combine to drive strong upwelling in the Agulhas current. *Journal of Physical Oceanography*, *47*(1), 123–134. https://doi.org/10.1175/JPO-D-16-0079.1

Leblanc, K., Hare, C. E., Boyd, P. W., Bruland, K. W., Sohst, B., Pickmere, S., et al. (2005). Fe and Zn effects on the Si cycle and diatom community structure in two contrasting high and low-silicate HNLC areas. *Deep-Sea Research Part A Oceanographic Research Papers*, *52*(10), 1842–1864. https://doi.org/10.1016/j.dsr.2005.06.005

Leles, S. G., & Levine, N. M. (2023). Mechanistic constraints on the trade-off between photosynthesis and respiration in response to warming. *Science Advances*, *9*(35). https://doi.org/10.1126/sciadv.adh8043

Le Moigne, F. A. C., Boye, M., Masson, A., Corvaisier, R., Grossteffan, E., Guéneugues, A., & Pondaven, P. (2013). Description of the biogeochemical features of the subtropical southeastern Atlantic and the Southern Ocean south of South Africa during the austral summer of the International Polar Year. *Biogeosciences*, *10*(1), 281–295. https://doi.org/10.5194/bg-10-281-2013

Lewis, S. L., & Maslin, M. A. (2015). Defining the Anthropocene. *Nature*, *519*(7542), 171–180. https://doi.org/10.1038/nature14258

Li, F., Ginoux, P., & Ramaswamy, V. (2008). Distribution, transport, and deposition of mineral dust in the Southern Ocean and Antarctica: Contribution of major sources. *Journal of Geophysical Research*, *113*(D10), D10207. https://doi.org/10.1029/2007JD009190

Li, G., Cheng, L., Zhu, J., Trenberth, K. E., Mann, M. E., & Abraham, J. P. (2020). Increasing ocean stratification over the past half-century. *Nature Climate Change*, *10*(12), 1116–1123. https://doi.org/10.1038/s41558-020-00918-2

Lin, L., He, J., Zhao, Y., Zhang, F., & Cai, M. (2012). Flow cytometry investigation of picoplankton across latitudes and along the Circum Antarctic Ocean. *Acta Oceanologica Sinica*, *31*(1), 134–142. https://doi.org/10.1007/s13131-012-0185-0

Liu, Y., King, H., van Huis, M., Drury, M., & Plümper, O. (2016). Nano-tomography of porous geological materials using focused ion beam-scanning electron microscopy. *Minerals (Basel)*, *6*(4), 104. https://doi.org/10.3390/min6040104

Lovecchio, S., Climent, E., Stocker, R., & Durham, W. M. (2019). Chain formation can enhance the vertical migration of phytoplankton through turbulence. *Science Advances*, *5*(10). https://doi.org/10.1126/sciadv.aaw7879

Mahowald, N. M., Kloster, S., Engelstaedter, S., Moore, J. K., Mukhopadhyay, S., McConnell, J. R., et al. (2010). Observed 20th century desert dust variability: Impact on climate and biogeochemistry. *Atmospheric Chemistry and Physics*, *10*, 10875–10893. https://doi.org/10.5194/acpd-10-12585-2010

Malkassian, A., Nerini, D., van Dijk, M. A., Thyssen, M., Mante, C., & Gregori, G. (2011). Functional analysis and classification of phytoplankton based on data from an automated flow cytometer. *Cytometry, Part A*, *79A*(4), 263–275. https://doi.org/10.1002/cyto.a.21035

Marchetti, A., & Harrison, P. J. (2007). Coupled changes in the cell morphology and elemental (C, N, and Si) composition of the pennate diatom *Pseudo-Nitzschia* due to iron deficiency. *Limnology & Oceanography*, *52*(5), 2270–2284. https://doi.org/10.4319/lo.2007.52.5.2270

Martin, J. H. (1990). Glacial-interglacial CO_2 change the iron hypothesis. *Paleoceanography*, *5*(1), 13. https://doi.org/10.1029/pa005i001p00001

Martin, P., Lampitt, R. S., Jane Perry, M., Sanders, R., Lee, C., & D'Asaro, E. (2011). Export and mesopelagic particle flux during a North Atlantic spring diatom bloom. *Deep-Sea Research Part A Oceanographic Research Papers*, *58*(4), 338–349. https://doi.org/10.1016/j.dsr.2011.01.006

Mayzel, B., Aram, L., Varsano, N., Wolf, S. G., & Gal, A. (2021). Structural evidence for extracellular silica formation by diatoms. *Nature Communications*, *12*(1), 4639. https://doi.org/10.1038/s41467-021-24944-6

Medlin, L. K., Kooistra, W. H. C. F., Sims, P., & Wellbrock, U. (1997). Is the origin of the diatoms related to the end-Permian mass extinction? *Nova Hedwig*, *65*, 1–11. https://doi.org/10.1127/nova.hedwigia/65/1997/1

Meredith, M., Sommerkorn, S., Cassota, S., Derksen, C., Ekaykin, A., Hollowed, A., et al. (2019). 2019: Polar regions. In *IPCC special report on the ocean and cryosphere in a changing Climate*.

Meyer, J., & Riebesell, U. (2015). Reviews and syntheses: Responses of coccolithophores to ocean acidification: A meta-analysis. *Biogeosciences*, *12*(6), 1671–1682. https://doi.org/10.5194/bg-12-1671-2015

Moore, J. K., Doney, S. C., Glover, D. M., & Fung, I. Y. (2001). Iron cycling and nutrient-limitation patterns in surface waters of the World Ocean. *Deep Sea Research Part II: Topical Studies in Oceanography*, *49*(1–3), 463–507. https://doi.org/10.1016/S0967-0645(01)00109-6

Morel, F. M. M. (1987). Kinetics of nutrient uptake and growth in phytoplankton. *Journal of Phycology*, *23*(1), 137–150. https://doi.org/10.1111/j.0022-3646.1987.00137.x

Morel, F. M. M., Hudson, R. J. M., & Price, N. M. (1991). Limitation of productivity by trace metals in the sea. *Limnology & Oceanography*, *36*(8), 1742–1755. https://doi.org/10.4319/lo.1991.36.8.1742

Morley, S. A., Griffiths, H. J., Barnes, D. K. A., & Peck, L. S. (2010). South Georgia: A key location for linking physiological capacity to distributional changes in response to climate change. *Antarctic Science*, *22*(6), 774–781. https://doi.org/10.1017/S0954102010000465

Mouw, C. B., Barnett, A., McKinley, G. A., Gloege, L., & Pilcher, D. (2016). Phytoplankton size impact on export flux in the global ocean. *Global Biogeochemical Cycles*, *30*(10), 1542–1562. https://doi.org/10.1002/2015GB005355

Nelson, D. M., Brzezinski, M. A., Sigmon, D. E., & Franck, V. M. (2001). A seasonal progression of Si limitation in the Pacific sector of the Southern Ocean. *Deep Sea Research Part II: Topical Studies in Oceanography*, *48*(19–20), 3973–3995. https://doi.org/10.1016/S0967-0645(01)00076-5

Nguyen, H., & Fauci, L. (2014). Hydrodynamics of diatom chains and semiflexible Fibres. *Journal of the Royal Society Interface*, *11*(96), 20140314. https://doi.org/10.1098/rsif.2014.0314

Nygaard, K., & Tobiesen, A. (1993). Bacterivory in algae: A survival strategy during nutrient limitation. *Limnology & Oceanography*, *38*(2), 273–279. https://doi.org/10.4319/lo.1993.38.2.0273

Patil, S. M., Mohan, R., Shetye, S. S., Gazi, S., Baumann, K.-H., & Jafar, S. (2017). Biogeographic distribution of extant coccolithophores in the Indian sector of the Southern Ocean. *Marine Micropaleontology*, *137*, 16–30. https://doi.org/10.1016/j.marmicro.2017.08.002

Perez-Garcia, O., Escalante, F. M. E., de Bashan, L. E., & Bashan, Y. (2011). Heterotrophic cultures of microalgae: Metabolism and potential products. *Water Research*, *45*, 11–36. https://doi.org/10.1016/j.watres.2010.08.037

Polyviou, D., Baylay, A. J., Hitchcock, A., Robidart, J., Moore, C. M., & Bibby, T. S. (2018). Desert dust as a source of iron to the globally important Diazotroph *Trichodesmium*. *Frontiers in Microbiology*, *8*, 2683. https://doi.org/10.3389/fmicb.2017.02683

Pörtner, H.-O., Roberts, D. C., Tignor, M., Poloczanska, E. S., Mintenbeck, K., Alegría, A., et al. (2022). *IPCC, 2022: Climate change 2022: Impacts, adaptation and vulnerability*. University Press Cambridge. 3056. https://doi.org/10.1017/9781009325844

Ras, J., Claustre, H., & Uitz, J. (2008). Spatial variability of phytoplankton pigment distributions in the subtropical south Pacific ocean: Comparison between in situ and predicted data. *Biogeosciences*, *5*(2), 353–369. https://doi.org/10.5194/bg-5-353-2008

Raven, J. A., & Geider, R. J. (1988). Temperature and algal growth. *New Phytologist*, *110*(4), 441–461. https://doi.org/10.1111/j.1469-8137.1988.tb00282.x

Redfield, A. C. (1934). On the proportions of organic derivatives in sea water and their relation to the composition of Plankton. *James Johnstone Memorial Volume, University Press of Liverpool*, 176–192.

Reinl, K. L., Harris, T. D., Elfferich, I., Coker, A., Zhan, Q., De Senerpont Domis, L. N., et al. (2022). The role of organic nutrients in structuring freshwater phytoplankton communities in a rapidly changing world. *Water Research*, *219*, 118573. https://doi.org/10.1016/j.watres.2022.118573

Riebesell, U., Fabry, V. J., Hansson, L., & Gattuso, J.-P. (2011). *Guide to best practices for ocean acidification research and data reporting*. Publications Office of the European Union.

Rigual-Hernández, A. S., Trull, T. W., Bray, S. G., & Armand, L. K. (2016). The fate of diatom valves in the Subantarctic and Polar Frontal Zones of the Southern Ocean: Sediment trap versus surface sediment assemblages. *Palaeogeography, Palaeoclimatology, Palaeoecology*, *457*, 129–143. https://doi.org/10.1016/j.palaeo.2016.06.004

Rodgers, K. B., Aumont, O., Mikaloff Fletcher, S. E., Plancherel, Y., Bopp, L., de Boyer Montégut, C., et al. (2014). Strong sensitivity of Southern Ocean carbon uptake and nutrient cycling to wind stirring. *Biogeosciences*, *11*(15), 4077–4098. https://doi.org/10.5194/bg-11-4077-2014

Saini, H., Kvale, K., Chase, Z., Kohfeld, K. E., Meissner, K. J., & Menviel, L. (2021). Southern Ocean ecosystem response to last glacial maximum boundary conditions. *Paleoceanography and Paleoclimatology*, *36*(7). https://doi.org/10.1029/2020PA004075

Schlosser, J. S., Braun, R. A., Bradley, T., Dadashazar, H., MacDonald, A. B., Aldhaif, A. A., et al. (2017). Analysis of aerosol composition data for western United States wildfires between 2005 and 2015: Dust emissions, chloride depletion, and most enhanced aerosol constituents. *Journal of Geophysical Research: Atmospheres*, *122*(16), 8951–8966. https://doi.org/10.1002/2017JD026547

Schuback, N., Hoppe, C. J. M., Tremblay, J., Maldonado, M. T., & Tortell, P. D. (2017). Primary productivity and the coupling of photosynthetic electron transport and carbon fixation in the Arctic Ocean. *Limnology & Oceanography*, *62*(3), 898–921. https://doi.org/10.1002/lno.10475

Schuback, N., Schallenberg, C., Duckham, C., Maldonado, M. T., & Tortell, P. D. (2015). Interacting effects of light and iron availability on the coupling of photosynthetic electron transport and CO_2-assimilation in marine phytoplankton. *PLoS One*, *10*(7), e0133235. https://doi.org/10.1371/journal.pone.0133235

Scott, F. J. & Marchant, H. J. (Eds.) (2005). Antarctic marine Protists, *Australian biological Resources study and Australian Antarctic division*.

Shi, C., Mao, R., Gong, D.-Y., Kim, S.-J., Feng, X., Sun, Y., & Dong, H. (2023). Increased dust transport from Patagonia to eastern Antarctica during 2000–2020. *Global and Planetary Change*, *227*, 104186. https://doi.org/10.1016/j.gloplacha.2023.104186

Shoenfelt, E. M., Winckler, G., Lamy, F., Anderson, R. F., & Bostick, B. C. (2018). Highly bioavailable dust-borne iron delivered to the Southern Ocean during glacial periods. *Proceedings of the National Academy of Sciences*, *115*(44), 11180–11185. https://doi.org/10.1073/pnas.1809755115

Shramik, P., Rahul, M., Suhas, S., & Sahina, G. (2013). Phytoplankton abundance and community structure in the Antarctic polar frontal region during austral summer of 2009. *Chinese Journal of Oceanology and Limnology*, *31*(1), 21–30. https://doi.org/10.1007/s00343-013-1309-x

Shukla, S. K., Crespin, J., & Crosta, X. (2016). *Thalassiosira lentiginosa* size variation and associated biogenic silica burial in the Southern Ocean over the last 42 kyrs. *Marine Micropaleontology*, *127*, 74–85. https://doi.org/10.1016/j.marmicro.2016.07.006

Smetacek, V., Klaas, C., Menden-Deuer, S., & Rynearson, T. A. (2002). Mesoscale distribution of dominant diatom species relative to the hydrographical field along the Antarctic Polar Front. *Deep Sea Research Part II: Topical Studies in Oceanography*, *49*(18), 3835–3848. https://doi.org/10.1016/S0967-0645(02)00113-3

Smetacek, V., Klaas, C., Strass, V. H., Assmy, P., Montresor, M., Cisewski, B., et al. (2012). Deep carbon export from a Southern Ocean iron-fertilized diatom bloom. *Nature*, *487*(7407), 313–319. https://doi.org/10.1038/nature11229

Strzepek, R. F., Maldonado, M. T., Hunter, K. A., Frew, R. D., & Boyd, P. W. (2011). Adaptive strategies by Southern Ocean phytoplankton to lessen iron limitation: Uptake of organically complexed iron and reduced cellular iron requirements. *Limnology & Oceanography*, *56*(6), 1983–2002. https://doi.org/10.4319/lo.2011.56.6.1983

Sugie, K., Nishioka, J., Kuma, K., Volkov, Y. N., & Nakatsuka, T. (2013). Availability of particulate Fe to phytoplankton in the sea of Okhotsk. *Marine Chemistry*, *152*, 20–31. https://doi.org/10.1016/j.marchem.2013.03.005

Sweetman, A. K., Thurber, A. R., Smith, C. R., Levin, L. A., Mora, C., Wei, C.-L., et al. (2017). Major impacts of climate change on deep-sea benthic ecosystems. *Elementa: Science of the Anthropocene.*, *5*, 4. https://doi.org/10.1525/elementa.203

Tagliabue, A., Bopp, L., Dutay, J.-C., Bowie, A. R., Chever, F., Jean-Baptiste, P., et al. (2010). Hydrothermal contribution to the oceanic dissolved iron inventory. *Nature Geoscience*, *3*(4), 252–256. https://doi.org/10.1038/ngeo818

Thyssen, M., Grégori, G., Créach, V., Lahbib, S., Dugenne, M., Aardema, H. M., et al. (2022). Interoperable vocabulary for marine microbial flow cytometry. *Frontiers in Marine Science*, *9*, 975877. https://doi.org/10.3389/fmars.2022.975877

Timmermans, K. R., Gerringa, L. J. A., de Baar, H. J. W., van der Wagt, B., Veldhuis, M. J. W., de Jong, J. T. M., et al. (2001). Growth rates of large and small Southern Ocean diatoms in relation to availability of iron in natural seawater. *Limnology & Oceanography*, *46*, 260–266. https://doi.org/10.4319/lo.2001.46.2.0260

Timmermans, K. R., & Van Der Wagt, B. (2010). Variability in cell size, nutrient depletion, and growth rates of the southern ocean diatom *fragilariopsis kerguelensis* (Bacillariophyceae) after prolonged iron limitation. *Journal of Phycology*, *46*(3), 497–506. https://doi.org/10.1111/j.1529-8817.2010.00827.x

Tomas, C. R. (1997). *Identifying marine phytoplankton*. Academic Press.

Tréguer, P., Bowler, C., Moriceau, B., Dutkiewicz, S., Gehlen, M., Aumont, O., et al. (2018). Influence of diatom diversity on the ocean biological carbon pump. *Nature Geoscience*, *11*(1), 27–37. https://doi.org/10.1038/s41561-017-0028-x

Tremblay, L., Caparros, J., Leblanc, K., & Obernosterer, I. (2015). Origin and fate of particulate and dissolved organic matter in a naturally iron-fertilized region of the Southern Ocean. *Biogeosciences*, *12*(2), 607–621. https://doi.org/10.5194/bg-12-607-2015

Trimborn, S., Brenneis, T., Hoppe, C., Laglera, L., Norman, L., Santos-Echeandía, J., et al. (2017). Iron sources alter the response of Southern Ocean phytoplankton to ocean acidification. *Marine Ecology Progress Series*, *578*, 35–50. https://doi.org/10.3354/meps12250

Trimborn, S., Brenneis, T., Sweet, E., & Rost, B. (2013). Sensitivity of Antarctic phytoplankton species to ocean acidification: Growth, carbon acquisition, and species interaction. *Limnology & Oceanography*, *58*(3), 997–1007. https://doi.org/10.4319/lo.2013.58.3.0997

Trimborn, S., Thoms, S., Brenneis, T., Heiden, J. P., Beszteri, S., & Bischof, K. (2017). Two Southern Ocean diatoms are more sensitive to ocean acidification and changes in irradiance than the prymnesiophyte *Phaeocystis antarctica*. *Physiologia Plantarum*, *160*(2), 155–170. https://doi.org/10.1111/ppl.12539

Tukey, J. W. (1949). Comparing individual means in the analysis of variance. *Biometrics*, *5*(2), 99. https://doi.org/10.2307/3001913

Tulet, P., Van Baelen, J., Bosser, P., Brioude, J., Colomb, A., Goloub, P., et al. (2024). MAP-IO: An atmospheric and marine observatory program on board *marion Dufresne* over the Southern Ocean. *Earth System Science Data*, *16*(8), 3821–3849. https://doi.org/10.5194/essd-16-3821-2024

Uitz, J., Claustre, H., Gentili, B., & Stramski, D. (2010). Phytoplankton class-specific primary production in the world's oceans: Seasonal and interannual variability from satellite observations. *Global Biogeochemical Cycles*, *24*(3), 2009GB003680. https://doi.org/10.1029/2009GB003680

Uitz, J., Claustre, H., Morel, A., & Hooker, S. B. (2006). Vertical distribution of phytoplankton communities in open Ocean: An assessment based on surface chlorophyll. *Journal of Geophysical Research*, *111*(C8), C08005. https://doi.org/10.1029/2005JC003207

Visser, P. M., Verspagen, J. M. H., Sandrini, G., Stal, L. J., Matthijs, H. C. P., Davis, T. W., et al. (2016). How rising CO_2 and global warming may stimulate harmful cyanobacterial blooms. *Harmful Algae*, *54*, 145–159. https://doi.org/10.1016/j.hal.2015.12.006

Weir, I., Fawcett, S., Smith, S., Walker, D., Bornman, T., & Fietz, S. (2020). Winter biogenic silica and diatom distributions in the Indian sector of the Southern Ocean. *Deep-Sea Research Part A Oceanographic Research Papers*, *166*, 103421. https://doi.org/10.1016/j.dsr.2020.103421

Weis, J., Chase, Z., Schallenberg, C., Strutton, P. G., Bowie, A. R., & Fiddes, S. L. (2024). One-third of Southern Ocean productivity is supported by dust deposition. *Nature*, *629*(8012), 603–608. https://doi.org/10.1038/s41586-024-07366-4

Wells, M. L., & Goldberg, E. D. (1993). Colloid aggregation in seawater. *Marine Chemistry*, *41*(4), 353–358. https://doi.org/10.1016/0304-4203(93)90267-R

Whitehouse, M. J., Priddle, J., & Symon, C. (1996). Seasonal and annual change in seawater temperature, salinity, nutrient and chlorophyll a distributions around South Georgia, South Atlantic. *Deep-Sea Research Part A Oceanographic Research Papers*, *43*(4), 425–443. https://doi.org/10.1016/0967-0637(96)00020-9

Wickham, H., Chang, W., Henry, L., Pedersen, T. L., Takahashi, K., Wilke, C., et al. (2007). ggplot2: Create elegant data visualisations using the Grammar of graphics [Software]. *CRAN: Contributed Packages*. https://doi.org/10.32614/CRAN.package.ggplot2

Winter, A., Henderiks, J., Beaufort, L., Rickaby, R. E. M., & Brown, C. W. (2014). Poleward expansion of the coccolithophore *Emiliania huxleyi*. *Journal of Plankton Research*, *36*(2), 316–325. https://doi.org/10.1093/plankt/fbt110

WoRMS Editorial Board. (2023). World register of marine species. https://doi.org/10.14284/170

Wu, Y., Campbell, D. A., Irwin, A. J., Suggett, D. J., & Finkel, Z. V. (2014). Ocean acidification enhances the growth rate of larger diatoms. *Limnology & Oceanography*, *59*(3), 1027–1034. https://doi.org/10.4319/lo.2014.59.3.1027

Wyatt, N. J., Birchill, A., Ussher, S., Milne, A., Bouman, H. A., Shoenfelt Troein, E., et al. (2023). Phytoplankton responses to dust addition in the Fe–Mn co-limited eastern Pacific sub-Antarctic differ by source region. *Proceedings of the National Academy of Sciences*, *120*(28), e2220111120. https://doi.org/10.1073/pnas.2220111120

Xiuren, N., Zilin, L., Genhai, Z., & Junxian, S. (1996). Size-fractionated biomass and productivity of phytoplankton and particulate organic carbon in the southern ocean. *Polar Biology*, *16*, 1–11. https://doi.org/10.1007/BF02388729

Zhang, Y., Collins, S., & Gao, K. (2020). Reduced growth with increased quotas of particulate organic and inorganic carbon in the coccolithophore *Emiliania huxleyi* under future ocean climate change conditions. *Biogeosciences*, *17*(24), 6357–6375. https://doi.org/10.5194/bg-17-6357-2020

Zhu, Z., Xu, K., Fu, F., Spackeen, J., Bronk, D., & Hutchins, D. (2016). A comparative study of iron and temperature interactive effects on diatoms and *Phaeocystis antarctica* from the Ross Sea, Antarctica. *Marine Ecology Progress Series*, *550*, 39–51. https://doi.org/10.3354/meps11732